REVISION AND PHYLOGENETIC ANALYSIS OF THE NORTH AMERICAN ANTLION GENUS *PARANTHACLISIS* BANKS (NEUROPTERA: MYRMELEONTIDAE)

A Thesis

by

BENJAMIN ROBERT DIEHL

Submitted to the Office of Graduate Studies of
Texas A&M University
in partial fulfillment of the requirements for the degree of

MASTER OF SCIENCE

August 2012

Major Subject: Entomology

Revision and Phylogenetic Analysis of the North American Antlion Genus

Paranthaclisis Banks (Neuroptera: Myrmeleontidae)

REVISION AND PHYLOGENETIC ANALYSIS OF THE NORTH AMERICAN ANTLION GENUS *PARANTHACLISIS* BANKS (NEUROPTERA: MYRMELEONTIDAE)

A Thesis

by

BENJAMIN ROBERT DIEHL

Submitted to the Office of Graduate Studies of
Texas A&M University
in partial fulfillment of the requirements for the degree of

MASTER OF SCIENCE

Approved by:

Chair of Committee,	John D. Oswald
Committee Members,	Gary Voelker
	James B. Woolley
Head of Department,	David W. Ragsdale

August 2012

Major Subject: Entomology

ABSTRACT

Revision and Phylogenetic Analysis of the North American Antlion Genus *Paranthaclisis* Banks (Neuroptera: Myrmeleontidae). (August 2012)

Benjamin Robert Diehl, B.A., The Ohio State University.

Chair of Advisory Committee: Dr. John D. Oswald

The North American antlion genus *Paranthaclisis* is comprehensively revised for the first time. Four species are recognized: *P. congener* (Hagen), *P. floridensis* Stange & Miller, *P. hageni* (Banks) and *P. nevadensis* Banks. Redescriptions, distribution maps and figures of diagnostic morphological characters are provided for adults of each species. A key to adults of *Paranthaclisis* is also included. *Paranthaclisis californica* Navás (1922) is recognized as a new synonym of *P. hageni* Banks. The monophyly of, and interspecific relationships within, the antlion genus *Paranthaclisis*, and its relationships to other genera within the tribe Acanthaclisini, are investigated using multiple datasets. Fifteen datasets were produced and analyzed to explore the effects of inference method, alignment strategy and data partitioning on phylogenetic estimates using morphological, molecular and mixed data inputs. Eighteen unordered and unweighted morphological characters were coded from across adult body regions. Molecular sequence data generated for this study consisted of two ribosomal genes, 16S and 18S. *Paranthaclisis* was recovered as monophyletic in analyses using 14 of 15 datasets, with low to moderate support in maximum parsimony and maximum likelihood

analyses and high support from Bayesian inference methods. A sister-group relationship between *Paranthaclisis* and *Vella*, the only other New World acanthaclisine genus, was also recovered in analysis of 13 of 15 datasets, with low to moderate support in all phylogenetic inference methods tested. Choice of phylogenetic inference method and partitioning of gene datasets had the most influence on resulting topologies and support values. Choice of alignment strategy resulted in few topological differences, but Clustal datasets generally had higher clade support values, compared to MAFFT-aligned sequences.

DEDICATION

To my parents,
Gerald and Linda Diehl

ACKNOWLEDGEMENTS

I would like to thank my committee chair and advisor, Dr. Oswald, for the opportunity to pursue a degree under his guidance and for all the hours of his invaluable advice and training. I would also like to thank my other committee members, Dr. Voelker and Dr. Woolley, for their assistance during my research and in the completion of this thesis.

Thanks also to the faculty, staff, and fellow students in the Texas A&M entomology department for their excellent teaching, assistance and help in making my time here as a M.S. student enjoyable. I would like to specifically thank the members of the Oswald, Light and Voelker laboratories for taking the time to help me during my research. I express my gratitude to the U. S. National Science Foundation, for supporting my graduate research under a Research Assistantship funded through a PEET (Partnerships for Enhancing Expertise in Taxonomy) grant.

I would also like to thank my family, for without them, none of this would have ever been possible. It was mainly through your continued support, and acceptance of my strange fascination with insects, that I had the confidence to pursue a professional career in the field that I enjoy so much. My earliest memories of exploring the natural world with my parents, sisters, and grandparents remain among my fondest, and I am very grateful to have had such a loving family.

Finally, I would like to thank Laura Ann McLoud for her constant support, love and determination for me to retain my sanity throughout this process, even when I did not feel it necessary myself.

TABLE OF CONTENTS

Page

LIST OF FIGURES

FIGURE Page

LIST OF TABLES

1. INTRODUCTION

The antlions or "doodlebugs" (Neuroptera: Myrmeleontidae) are a group of medium to large-sized lacewings with elongate, slender, bodies and prominent, sub-equal wings. The family is cosmopolitan in distribution (New 1989), and displays high diversity in areas such as southern Africa, Australia and the southwestern United States (New 1986). Antlions are particularly numerous and speciose in dry areas characterized by deep sand or fine, loamy soils, due to the preference for these habitats by their immature stages. The family is well known for species with larvae that build conical pits in loose substrates to aid in the capture of prey, although this pit-building behavior is found in less than half of all antlion species and is mostly restricted to one tribe. Non-pit-building larvae are known to inhabit a variety of microhabitats, including tree-hole cavities (Miller and Stange 1983), caves (Stange 1970b), animal burrows (Davis & Milstrey 1988, Stange 2000), rock faces (Stange 1970b), under tree bark (Stange 1980) and areas of deep sand (New 1986, Stange 1980, Stange & Miller 1985). Adult antlions have been noted as feeding on small insects and pollen, whereas larvae are entirely predaceous on small arthropods. Studies of the behavior and ecological characteristics of the larvae of pit-dwelling antlions are numerous (McClure 1976, Allen & Croft 1985, Napolitano 1998, Dias et al. 2006, Hollis et al. 2011), but little is known of the biologies of non-pit-building larvae, and even basic biological information, such as mating and ovipositon strategies, is largely unknown for the adults of most taxa.

This thesis follows the style of Annals of the Entomological Society of America.

The family Myrmeleontidae currently contains over 1500 valid extant species worldwide in 191 genera (Stange 2004). In North America, 152 species are known, representing 22 genera (Stange 2004, Oswald 2009). The higher-level classification of the Myrmeleontidae has historically been problematic, with several authors proposing different taxonomic divisions at the subfamily, tribe and subtribe levels (Banks 1899, 1911, Navás 1912, Esben-Peterson 1918, Markl 1954, Stange 1970, 1976, 1994, New 1985a, 1985b, 1985c). More than 7 subfamilies and 33 tribes have been proposed within the Myrmeleontidae during the past century, but inadequate descriptions, lack of detailed illustrations, and the existence of few broad comparative studies have made interpreting taxa and phylogenetic relationships difficult (Mansell 1985). In his recent world monograph of the Myrmeleontidae, Stange (2004) recognized 3 subfamilies (Stilbopteryginae, Palparinae, and Myrmeleontinae) and 14 tribes (Palparidiini, Palaprini, Pseudimarini, Dimarini, Maulini, Dendroleontini, Nemoleontini, Brachynemurini, Gnopholeontini, Lemolemini, Myrmecaelurini, Nesoleontini, Myrmeleontini and Acanthaclisini) based on adult and larval morphologies. Of the 191 valid antlion genera recognized by Stange (2004), 169 are included within Myrmeleontinae, 20 within Palparinae and 2 in Stilbopteryginae. Tribal groupings vary considerably across the Myrmeleontidae in the number of included genera and species, with some containing over 100 species and others fewer than five. Supergeneric classifications of antlions are based largely on differences in wing venation, believed to be a slowly evolving character complex and hypothesized to provide stable higher-level groupings (Stange 2004). Venational characters have also been used extensively to

differentiate taxa at the genus level, but other anatomical features, such as male and female terminalia, have also been important. Species-level classifications have employed a wide range of character suites to diagnose taxa, but identifications can be difficult when based solely on sex-specific morphologies, color patterns that display intraspecific variation, or generalized length or width measurements of particular structures.

The genus *Paranthaclisis* Banks currently contains four valid species, which are collectively restricted to the western and southern United States and northern Mexico. The genus *Paranthaclisis* was erected by Banks (1907) for two North American species then placed in the genus *Acanthaclisis* Rambur; *Acanthaclisis congener* Hagen, type species, and *Acanthaclisis hageni* Banks. Navás (1919, 1922) described two taxa, with different descriptions and types, under the name *Paranthaclisis californica*; the former was considered a junior synonym of *Paranthaclisis hageni* by Stange (2004). Banks (1939) described a third species, *Paranthaclisis nevadensis*, and Stange & Miller (2012) most recently described *Paranthaclisis floridensis* from Florida.

Adults of *Paranthaclisis* are thick-bodied, hairy antlions and its species have been differentiated on the basis of morphological differences of the head, mesoscutum, abdominal tergites and male terminalia. Larvae are found in areas of deep sand, including coastal and inland desert dunes, and lack the pit-building behavior for which the family is popularly known. Instead, *Paranthaclisis* larvae actively pursue prey through rapid backward movements while remaining completely buried beneath the sand (Stange & Miller 1985). Once within reach of a potential prey item, larvae strike upwards to grab small arthropods and pull them under the surface of the sand.

Paranthaclisis is one of two acanthaclisine genera found in the New World. It can be differentiated from the second genus, *Vella* Navás, by the presence, in *Paranthaclisis*, of strongly angled [not gently curved] tibial spurs, a scarcely pedicellate [not strongly pedicellate] labial palpomere and a predominantly uniareolate [not predominantly biareolate] forewing costal area adjacent to the pterostigma (Stange & Miller 1985). The monophyly of *Paranthaclisis* is supported by several putative morphological synapomorphies that distinguish it from other acanthaclisine genera (see Diagnosis of genus description below). Adults display distinctive hind wing venation in which the posterior fork of the MP_2 is joined to the CuA as a short decurved veinlet. *Paranthaclisis* larvae are also unique within the tribe Acanthaclisini in having only one tooth (not three) per mandible.

2. TAXONOMIC REVISION

2.1 Introduction

Revisionary treatments have recently been completed for several New World myrmeleontid taxa (Miller & Stange 1989, 2009, Stange 1970a, 1970b) at the tribal and generic levels. In this thesis, I expand upon the taxonomic studies of the family Myrmeleontidae by completing a revision of the North American genus *Paranthaclisis* Banks (Myrmeleontidae: Acanthaclisini). *Paranthaclisis* was briefly reviewed at the generic level by Stange & Miller (1985), and cataloged at the species level by Stange (2004), but it has never been the subject of a comprehensive revisionary treatment. In the following revision, four valid species are recognized in *Paranthaclisis*: *congener, floridensis*, *hageni* and *nevadensis*. Descriptions and diagnoses are provided for all adult male and female *Paranthaclisis* species, and available data concerning the distribution, synonymy, biology, immature stages, primary types, material examined and etymology of the species are synthesized. Photographs and illustrations of important diagnostic morphological characters are provided, including the first descriptions and illustrations of the male genitalia.

2.2 Materials and Methods

2.2.1 Material and Collection Acronyms

This revision is based on 1597 adult *Paranthaclisis* specimens examined from the following 11 collections: American Museum of Natural History, New York, NY,

U.S.A. (AMNH); Academy of Natural Sciences, Philadelphia, PA, U.S.A. (ANSP); California Academy of Natural Sciences, San Francisco, CA, U.S.A. (CAS); Florida State Collection of Arthropods, Gainesville, FL, U.S.A. (FSCA); Muséum National d'Histoire Naturelle, Paris, France (MNHN); Oregon State Arthropod Collection, Corvallis, OR, U.S.A. (OSAC); San Diego Natural History Museum, San Diego, CA, U.S.A. (SDMC); Texas A&M University, College Station, TX, U.S.A. (TAMU); University of Arizona, Tucson, AZ, U.S.A. (UAIC); Utah Museum of Natural History, Salt Lake City, UT, U.S.A. (UMNH); Maurice T. James Entomological Collection, Pullman, WA, U.S.A. (WSU).

2.2.2 Specimen Dissections

Dissections were conducted following the methodology outlined by Oswald (1993). In summary, terminalic and genitalic structures were macerated in a 10% KOH solution and stained with Chlorazol Black, then rinsed in 70% EtOH to remove macerated tissue and excess stain. Structures were suspended in glycerin for examination and illustration under a dissecting microscope.

2.2.3 Illustrations and Photographs

Drawings were made by hand on paper using an Olympus S2-PT dissecting microscope, then digitally scanned and edited using Adobe Photoshop (San Jose, California, USA). Photographs were taken with a Microptics Digital Imaging System using a Canon EOS 1D Mark IIn digital camera. To increase depth of field in

photographs, multiple stacked images were combined using the software CombineZP (available at: http://www.hadleyweb.pwp.blueyonder.co.uk/Index.htm).

2.2.4 Terminology

General entomological terminology follows that of Nichols (1989). Terminalic and genitalic terms follow Stange (1970) and Oswald (1993). Several specialized terms are discussed below:

Banksian lines. – The terminology of Banks (1927) and Stange (1970) is followed here, in which anterior and posterior Banksian lines are recognized in both the forewing and hind wing. Banksian lines are longitudinal vein traces formed in the forewing by aligned portions of successive branches of the radial sector (anterior Banksian line) and CuA (posterior Banksian line) and in the hind wing by aligned portions of successive branches of the radial sector (anterior Banksian line) and MP_2 (posterior Banksian line). The Banksian lines also include short crossveins that connect the aligned longitudinal vein segments. Banksian lines are linear flexion zones that bend during flight.

Eversible sacs of male abdomen. – New (1981) noted the presence of hair pencils, a term used to refer to similar structures in Lepidoptera, in several acanthaclisine genera. These structures have been linked to glandular systems in the male abdomen and are hypothesized to function in sexual signaling by aiding in the dispersal of volatile chemical signals (New 1981). Stage (2004) reported that all acanthaclisine antlion genera contain taxa that have hair pencils, except the Australian genus *Arcuaplectron*

New. He also noted that hair pencils, also termed eversible sacs (Stange 2012), were absent in *P. nevadensis*. There is some morphological variation in the structure of hair pencils within the Acanthaclisini. In *Cosina*, for example, there are numerous long setae that create the hair pencil or brush. *Paranthaclisis,* however, lacks these setae and the structure is present as an eversible membranous sac only. Although morphologically different in some acanthaclisine taxa, these structures all arise from the same position within the intertergal membrane between tergites 6 and 7 and therefore appear to be homologous.

Mesoscutellar rim. – The posterior margin of the dorsal surface of the mesoscutellum is strongly sclerotized and shining in all species of *Paranthaclisis*. The coloration of this structure is useful for distinguishing *P. congener* from other species in the genus.

Ocular rim setae. – The ocular rim was defined by Stange (1970) to be the narrow raised area immediately adjacent the inner margin of the eye. Setae that are sometimes present on the ocular rim often extend over the eye and have been used previously as diagnostic characters for recognizing taxa. Differences were observed in both the abundance and length of ocular rim setae in *Paranthaclisis*. Due to the tendency of ocular rim setae to break off during collecting or handling, this character is not generally useful for species identification. However, both the number and size of ocular rim setae in *P. congener* are smaller than other *Paranthaclisis* species.

Presectoral spurious vein. – This character was previously noted in the Acanthaclisini by Kimmins (1939), as an “accessory longitudinal veinlet”, by New

(1985) as a “spurious longitudinal vein”, and by Stange & Miller (1985) as an “accessory longitudinal vein”. Located in the presectoral area as defined by Stage (1970), this spurious vein runs parallel to the Radius for a short distance and connects two or more adjacent crossveins. In some taxa, the presectoral spurious vein does not connect any adjacent crossveins but is indicated by expansions on the lateral margins of adjacent crossveins in the presectoral area. Based on descriptions and figures in the literature, this character is present in at least one species of the following acanthaclisine genera: *Acanthaclisis*, *Arcuaplectron*, *Centroclisis*, *Fadrina*, *Heoclisis*, *Paranthaclisis*, and *Stiproneuria*.

2.2.5 Annotations

The following annotations are used in synonymical listings to indicate subject matter contained in cited literature: DN, distribution; FB, feeding biology; FG, figure; KA, adult key; KL, larva key; LA, larvae; LT, listed; NO, nomenclature; OD, original description; RB, reproductive biology; RD, redescription; TA, taxonomy.

2.2.6 Miscellaneous

Species are treated in alphabetical order. Body length measurements were taken from the anterior margin of the vertex markings to the posterior margin of tergite 7. Forewing and hind wing measurements were taken from the origin of the radius to the apex of the wing. All measurements were rounded to the nearest millimeter. Geographic distribution maps were generated using specimen locality data from only labels containing one or

more of the following: (1) latitude and longitude measurements, (2) a mile or kilometer distance measurement in relation to a named city, park, road intersection, etc., (3) unambiguous names of cities, parks or other landmarks. Adult activity ranges are based on the earliest and latest collecting dates recorded from label data. Non-type distributions were cited only to county (United States of America) or municipality (Mexico). Materials examined sections include all specimens acquired through institutional loans, as well as specimens identified and cataloged during visits to the CAS and FSCA. Per International Code of Zoological Nomenclature Article 8.2, this thesis in not issued for public and permanent scientific record or purposes of zoological nomenclature.

2.3 Genus *Paranthaclisis* Banks

Paranthaclisis Banks, 1907: 275. Type species: *Acanthaclisis congener* Hagen, 1861: 224, by the subsequent designation of Banks 1927: 80. Hagen 1887:151 (LA); Banks 1913: 149 (TA); Banks 1927: 79-80 (FG- adult tibial spur, adult labial palp, KA, RD, TA); Banks1939: (KA, TA); Stange 1970: 20-21, 24, 43 (KL, LA); Stange 1980: 1-2 (FG- larva jaw, KL, LA); New 1981: 375 (TA); Stange & Miller 1985: 29-32, 34, 36-38, 40, 42 (FG- larva abdomen, KA, KL, LA, RB, TA); Stange 1994: 70 (LA); Stange 2004: 15, 340, 355-356, 387, 393 (DN, KA, KL, LA, NO, TA); Bezzi et al. 2010: 2237 (LT); Gepp 2010: 48 (LA); Stange & Miller 2012: 1-3 (DN, FB, KA, KL, LA, NO, RB, RD, TA).

2.3.1 Diagnosis

One of only two acanthaclisine genera known from the New World. *Paranthaclisis* can be differentiated from the second genus, *Vella* Navás, by the presence in *Paranthaclisis* [non-*Paranthaclisis* state(s) in square brackets] of strongly angled [not evenly curved] tibial spurs, a forewing costal area that is predominantly uniareolate adjacent to the pterostigma [not partially biareolate], a scarcely pedicellate labial palpomere [not strongly pedicellate], and male ectoproct with postventral lobe length 2 to 3 1/2 times width at midpoint [not > 4 times width at midpoint]. Distinguished from other genera of the Acanthaclisini by the following combination of adult characters in *Paranthaclisis*: (1) posterior fork of MP_2 is joined to CuA as a short decurved veinlet in hind wing [not running subparallel to, before fusing with, CuA], (2) tibial spurs acutely bent at midpoint [not evenly curved], proximal half of spur with laterally compressed flange ventrally, (3) forewing costal area predominantly uniareolate adjacent to pterostigma [not biareolate], (4) pro-, meso- and metafemora each with one elongate sense hair [not two], (5) male abdomen with eversible sacs present (except *P. nevadensis*) [not absent] dorsolaterally in intertergal membrane between tergites 6 and 7.

2.3.2 Description

Body length: 26 – 39 mm (mean = 32, n = 181); *forewing length*: 29 – 43 mm (mean = 34, n = 181); *hind wing length*: 27 – 40 mm (mean = 32, n = 181).

2.3.2.1 Head

Frons: bearing setae longer than length of scape; *antenna*: clavate, flagellomeres dark brown, distal margins pale; *labrum*: distal palpomere of labial palp swollen, opening to sensory area marked by sagittal slit spanning distal 2/3 of outer face; *vertex markings*: covering most of vertex, with or without setae; *ocular rim*: ocular rim setae present, running in a continuous or broken band from posterior margin of vertex markings to antenna.

2.3.2.2 Thorax

Pronotum: wider than long, lateral margins with long anteriorly-arched setae; *mesoscutum*: bearing long setae; *mesoscutellum*: mesoscutellar rim strongly sclerotized, shining.

2.3.2.3 Wings (fig. 1a)

General: forewing and hind wing (at rest) longer than abdomen; *forewing*: shape: apex acuminate; coloration: wing cells mostly hyaline, but with dark brown margining adjacent to darkly-colored vein segments or darkly-colored longitudinal vein segments only; longitudinal veins with alternating dark and pale regions; crossveins mostly dark brown or with alternating light/dark pattern, fewer entirely pale; venation: costal area uniareolate throughout or uniareolate proximally and biareolate distally (in *P. floridensis*) adjacent to pterostigma; pterostigma dark brown to black, yellowish white distally; presectoral area with 6-8 crossveins; Rs arising in basal 1/3 of wing, but distal

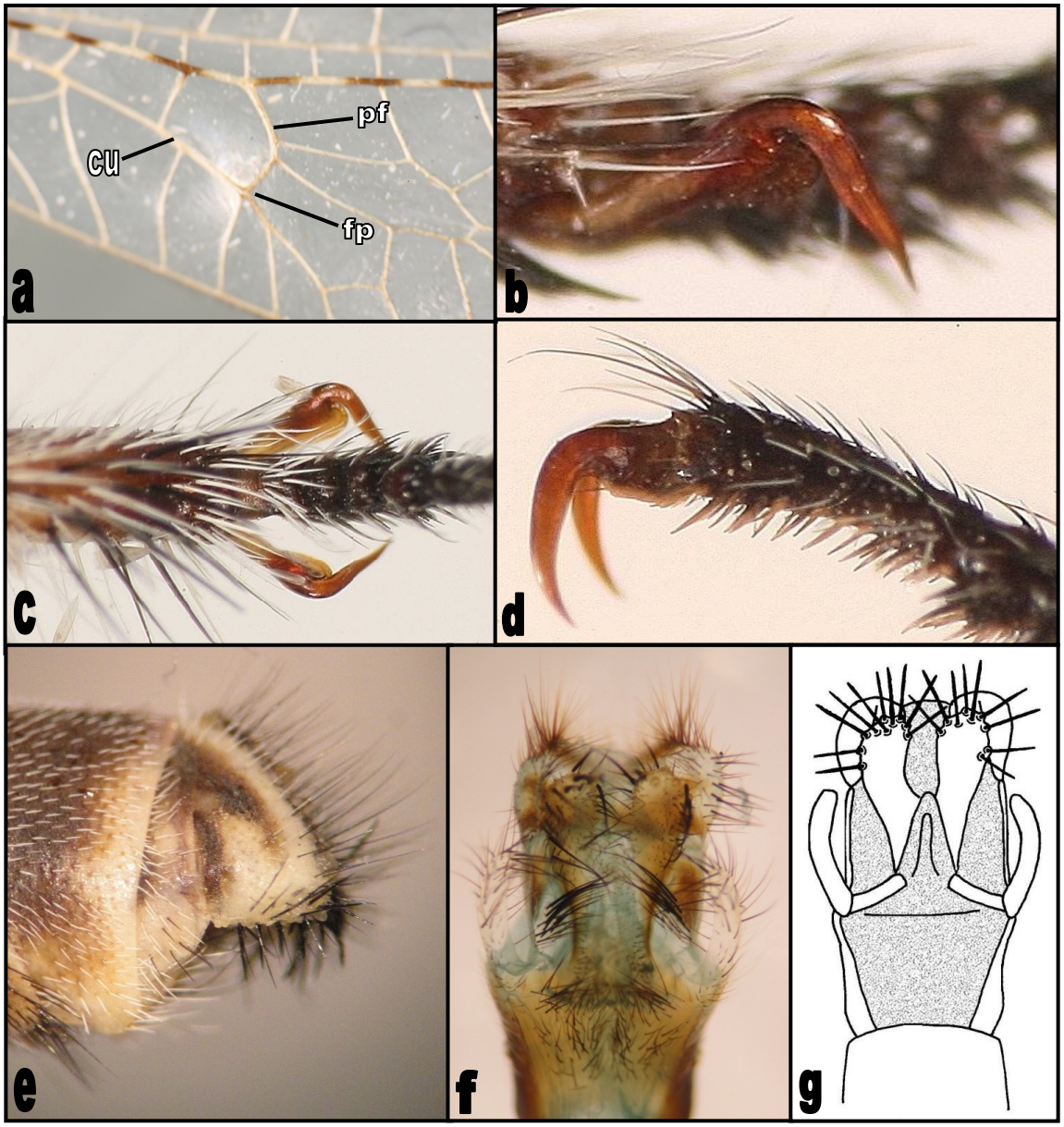

Fig. 1. *Paranthaclisis sp.*, diagnostic characters. a, hindwing, ; b, tibial spur, lateral; c, tibial spurs, dorsal; d, pretarsal claws, lateral; e, female terminalia, lateral; f, female terminalia, ventral; g, female terminalia, lateral. Abbreviations: cu – CuA vein; fp – fusion point; pf – posterior fork MP_2.

to cubital fork; CuP arising near basal crossvein; anterior and posterior Banksian lines well defined; *hind wing*: apex acuminate; longitudinal veins with alternating dark brown and pale regions; crossveins mostly pale or with alternating light/dark pattern, fewer entirely dark brown; costal area uniareolate adjacent to pterostigma; pterostigma dark brown to black, yellowish white distally; presectoral area with 5-7 crossveins; presectoral spurious vein connecting at two or more presectoral crossveins, or indicated only as expansions on lateral margins of some crossveins; Rs arising in basal 1/3 of hind wing, but distal to medial fork; posterior fork of MP_2 fusing with CuA as short decurved veinlet; anterior and posterior Banksian lines well defined; *male*: pilula axilaris well developed, about as long as wide, distal half of dorsal face densely covered with fine golden setae.

2.3.2.4 Legs (figs. 1b-d)

General: proleg and mesoleg similar in length, metaleg longer; dorsal surface of all femora brown; dorsal surface of all tibiae banded with alternating brown and pale regions; ventral faces of all leg segments brown or pale; all legs densely covered with long white setae; *proleg*: profemur slightly swollen compared to meso- and metafemur, with one femoral sense hair, sense hair ≥ length of profemur, ventral face of profemur with 3-4 rows of stout black spines, spine length ≤1/2 width of profemur, ventral face of protibia with a series of short black setae, setae length gradually increasing distally; distal 1/4 of ventral surface of protibia with patch of short, dense, golden setae (antennal cleaning structure), expanding along inner posterolateral surface to cover portion of

dorsal face; *mesoleg*: with one femoral sense hair, sense hair ≥ length of mesofemur; ventral face of mesofemur with 3-4 rows of stout black spines, spine length ≤1/2 width of mesofemur; ventral face of mesotibia with a series of short black setae, setae length gradually increasing distally on tibia; *metaleg*: with one femoral sense hair, sense hair ≤ 3/4 length of metafemur; ventral face of metafemur with 3-4 rows of stout black spines, length of some spines > 1/2 width of metafemur; ventral face of metatibia with series of short black setae, gradually increasing in length distally; *tibial spurs*: present, bent ca. 90˚ near midpoint, base to tip of spur as long as basal four tarsomeres, proximal half with laterally compressed flange ventrally; *tarsus*: distal tarsomere much longer than individual basal tarsomeres, shorter or longer than combined length of four basal tarsomeres; pretarsal claws acutely angled at proximal 1/3, total length of claw around angle shorter than distal tarsomere.

2.3.2.5 Abdomen

General: tergites entirely dark gray, or posterior margins with a transverse, pale band (pale area expanded anteriorly on some segments in some species); with short, white pilosity; all segments densely covered with long black setae and long white setae; *male*: with a pair of eversible sacs present dorsolaterally in intertergal membrane between tergites 6 and 7, (sacs absent in *nevadensis*).

2.3.2.6 Male terminalia

9th tergite: divided sagittally, hemi tergites rectangular, 1/3 length of tergite 8,; *9th sternite*: posterior margin rounded, prow-shaped, projecting slightly beyond tergite 9, posterior margin with several long black setae and long white setae; *ectoproct*: postventral lobe directed ventrally, sub cylindrical, apex rounded, lobe length 2 to 3 1/2 times width at midpoint, < length of tergite 8.

2.3.2.7 Male genitalia

Gonarcus: extragonarcus a transverse plate with a widely bifurcated posterior margin, posterior face of extragonarcus proximal to mediuncus shallowly or deeply invaginated in lateral view; intragonarcus developed as a pair of internal arms originating from anterolateral margins of extragonarcus, length of internal arm 2 to 3 times middle width, laterally compressed distally; *medincus*: length 2 to 3 1/2 times middle width, flexing relative to posterior face of extragonarcus beyond basal invagination of extragonarcus; in dorsal view, basal half broad, subparallel sided, apical half attenuate; *9th gonocoxites*: associated proximally with posterolateral margins of extragonarcus, membrane bounded (except for apical hooks), elongate, directed ventrally, with slightly recurved hooks at posteroventral margins, ventral surface of hooks spiculate.

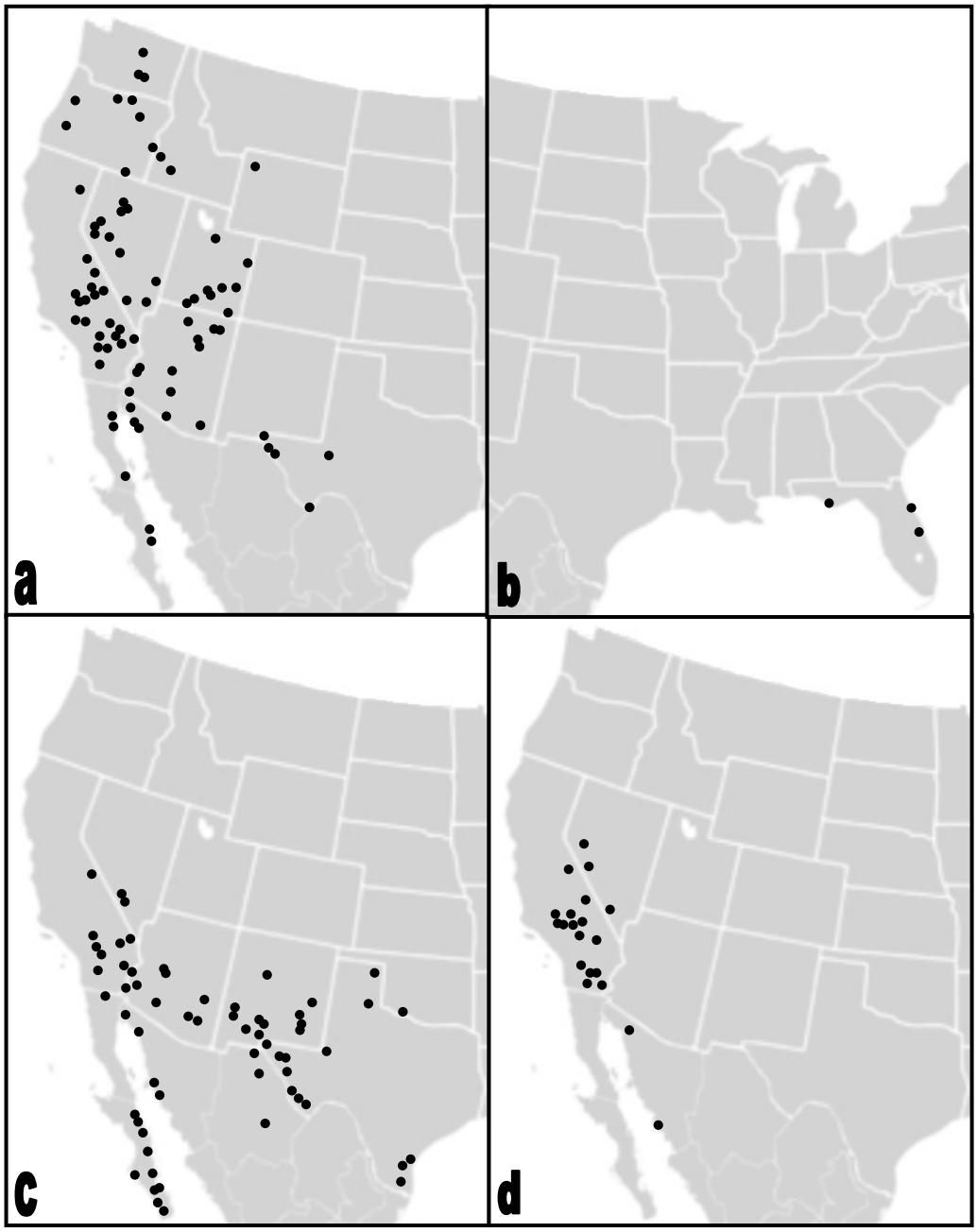

Fig. 2. Geographic distribution of *Paranthaclisis* species. a, *P. congener*; b, *P. floridensis*; c, *P. hageni*; d, *P. nevadensis*. Only personally examined specimens plotted.

2.3.2.8 Female terminalia (figs. 1e-g)

8th tergite: hemi annular; *9th tergite*: divided sagittally, hemi tergites rectangular; *pregenital plate*: absent; *posterior gonapophyses*: associated proximally with posterolateral margins of tergite 8, length 5 times width, bearing numerous long setae, many setae ≥ 2/3 posterior gonapophysis length; *gonapophyseal plate*: glabrous, running transversely from posterior gonapophyses to base of vulva; *lateral gonapophyses*: produced parasagittally posterior to vulva, thumb-like, shorter than posterior gonapophyses, length 1 1/2 to 2 times width, bearing 6-11 thickened digging setae; *ectoproct*: ovoid, with anterior margin straight, bearing numerous long dark brown setae and long white setae, postventral lobe absent.

2.3.3 Distribution (figs. 2a-d)

North America (United States of America and Mexico). Western United States of America (widespread, northern Washington east to Wyoming and south to southern California and western Texas), eastern United States of America (Gulf and Atlantic coasts of northern Florida), and northwestern Mexico (northern and southern Baja peninsula east to Chihuahua and south to Sinaloa).

2.3.4 Adult Activity Period

1 April – 22 November. All species most commonly collected from June through August.

2.3.5 Biology

Adult *Paranthaclisis* are nocturnal and can be readily collected using light sheets and traps. Adult feeding biology is unknown for the genus, but some species have been observed visiting flowers and potentially ingesting pollen or nectar. For specific biological information available for each species, see Biology under species descriptions.

2.3.6 Immature Stages

Larvae of all four species have been collected and reared in the laboratory by Lionel Stange and Bruce Miller. See Stange (2004) and Stange & Miller (1985, 2012) for descriptions of larvae and keys to *Paranthaclisis* and the genera of Acanthaclisini based on larval morphology. *Paranthaclisis* larvae are unique within the Acanthaclisini in possessing only one tooth on each mandible and having reduced antennae. In common with other antlions, *Paranthaclisis* larvae progress through three larval instars. Pupation occcurss under the sand in a spherical cocoon constructed of silk and sand grains. Diapause has not been studied in *Paranthaclisis*, but Stange & Miller (1985) suggest that if such a period occurs, it takes place in the larva, not in the eggs or pupa. The pupal period is approximately 54 days. Both forward and backward movement has been observed in *Paranthaclisis* larvae (Stange & Miller 1985). Larvae do not construct pit-fall traps but instead inhabit open tracts of deep sand, such as inland deserts and costal dunes. Surface prey is pursued by backward movements under the sand until the larvae can successfully reach up to grab the food item with its jaws. *Paranthaclisis* larvae have

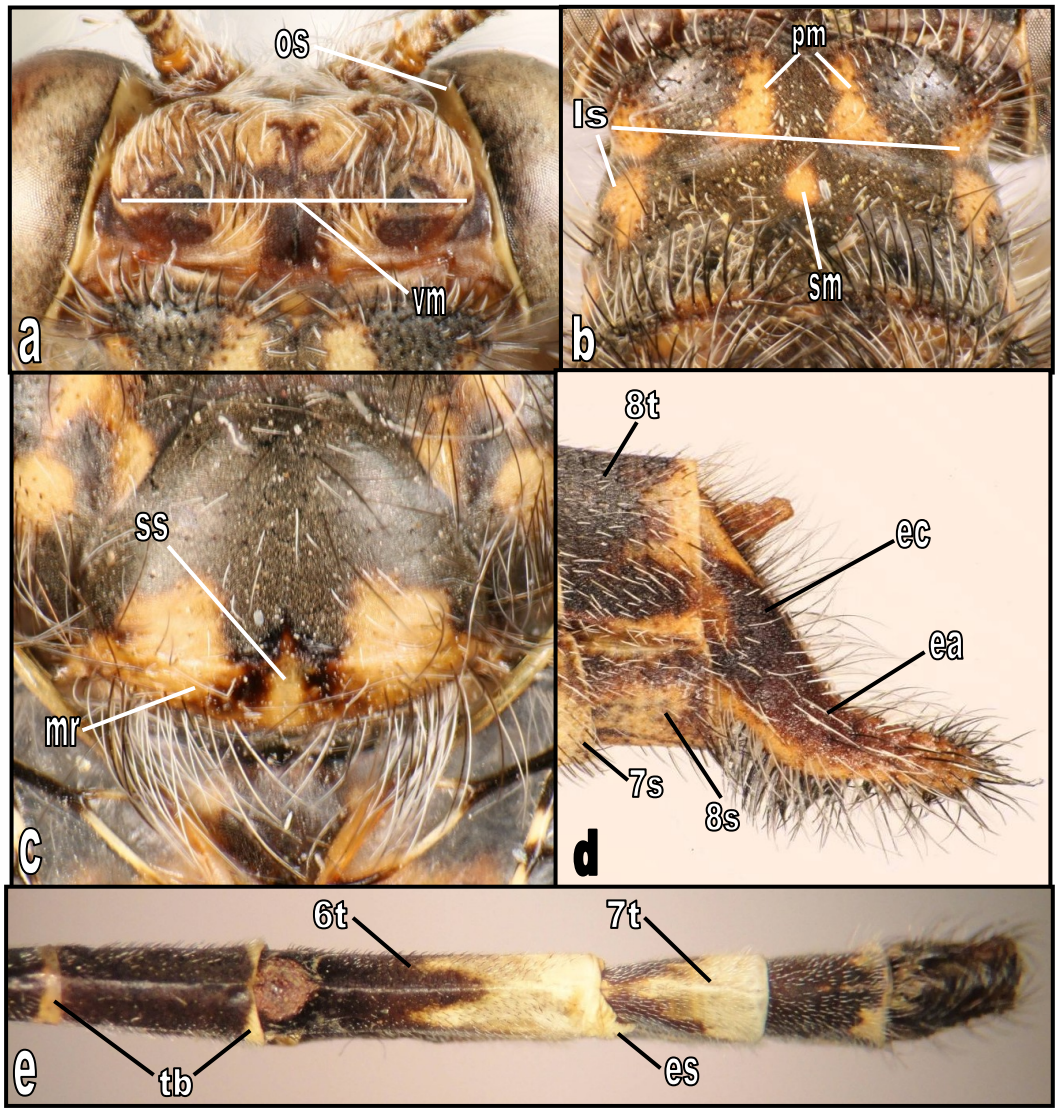

Fig. 3. *Paranthaclisis congener*, diagnostic characters. a, vertex, dorsal; b, pronotum, dorsal; c, mesothorax, dorsal; d, male abdomen, apex, lateral; e, male abdomen, dorsal. Abbreviations: 6t – 6th tergite; 7t – 7th tergite; 8s – 8th sternite; 8t – 8th tergite; ea – ectoproct angle; ec – ectoproct; es – eversible sac; ls – lateral stripe; mr – mesoscutellar rim; os – ocular rim setae; pm – parasagittal marks; sm – sagittal mark; ss – sagittal stripe of mesoscutellar rim; tb – transverse band; vm – vertex markings.

been observed feeding on Lepidoptera (butterflies and moths) larvae and adult Coleoptera (beetles).

2.3.7 Species (4)

(1) *congener*: United States of America, Mexico; (2) *floridensis*: United States of America; (3) *hageni*: United States of America, Mexico; (4) *nevadensis*: United States of America, Mexico.

2.3.8 Etymology

Unexplained in original description, probably Para- [from the Greek *para*, near] + -nthaclisis [from *Acanthaclisis,* the genus in which the type species was originally described], in reference to the taxonomic status of *Paranthaclisis* as a group closely related to, but outside of *Acanthaclisis*.

2.4 *Paranthaclisis congener* (Hagen) (Figs. 2a, 3a-e, 4a-e)

Acanthaclisis congener Hagen, 1861:224 (OD). – Hagen 1860:363 (LS); Hagen 1866:378 (DN, LS); Hagen 1877:151-152, 154-155 (LV, RD); Banks 1892:360 (LS); Banks 1895:518 (DN); Banks 1899:170 (TA); Currie 1903:274 (DN).

Paranthaclisis congener (Hagen): Banks 1907a:275 (NO, TA); Banks 1907b:29 (LS); Banks 1927:80-81 (DN, KY, RD); Banks 1939:4-5 (FG- adult male terminalia, KY, MT, TA); Banks 1942:148 (LS, DN); Stange & Miller 1985:29, 37 (LA,

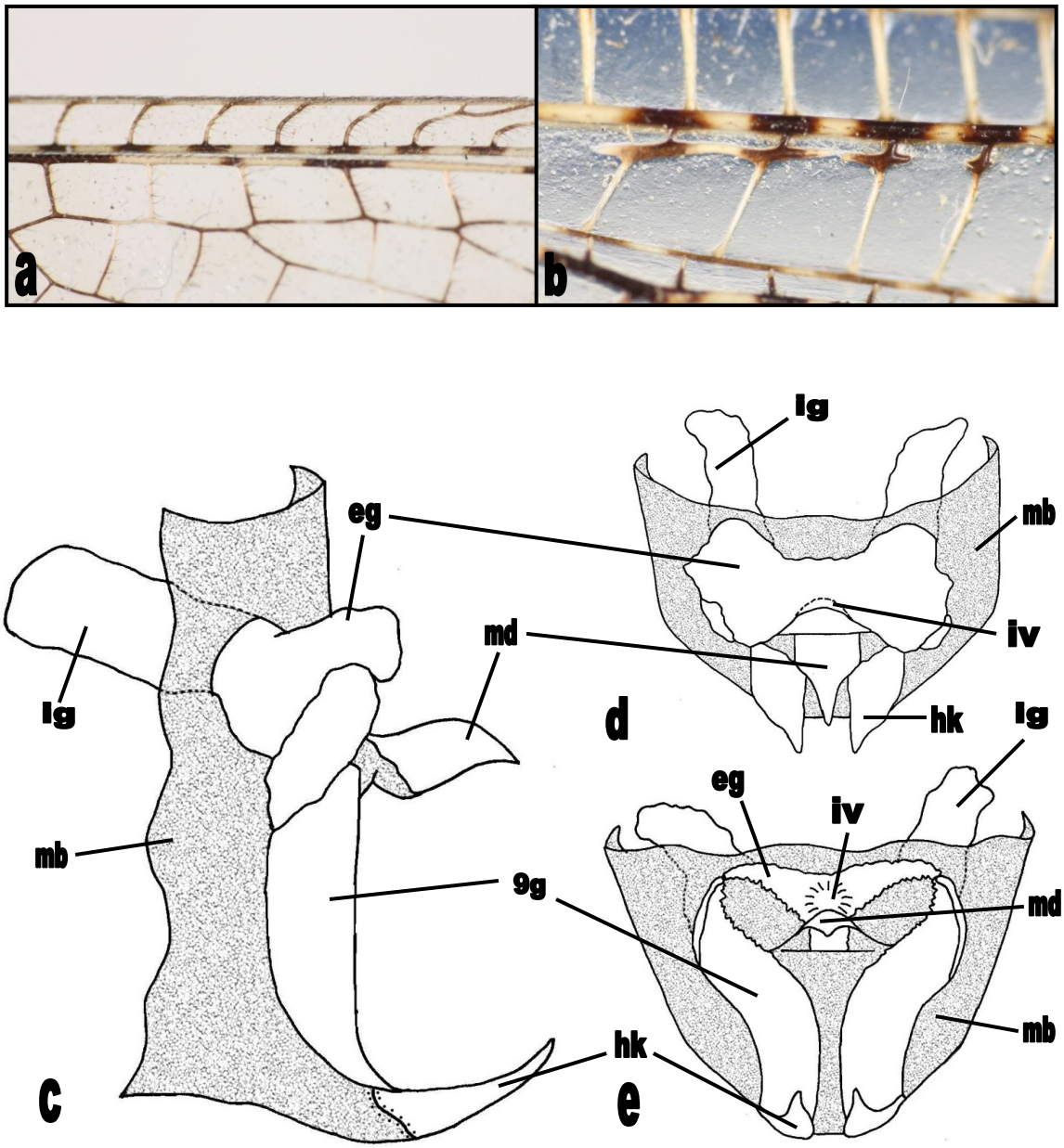

Fig. 4. *Paranthaclisis congener*, wings and male genitalia. a, forewing, costal area, dorsal; b, hind wing, presectoral area, dorsal; c, gonarcus complex, lateral; d, gonarcus complex, dorsal; e, gonarcus complex, posterior. Abbreviations: 9g – 9th gonocoxite; ex – extragonarcus; hk – apex of gonocoxite 9; ig – intragonarcus; iv – invagination of extragonopons; mb – membrane; md – mediuncus.

RB); New 1986:26 (RB); Penny et al. 1997:75 (DN, LS, TY); Zack et al. 1998:207 (LS); Oswald et al. 2002:580 (LS); Stange 2004:356 (DN, TA, TY); Stange & Miller 2012:1-3, 5 (KY, LA).

2.4.1 Diagnosis

Distinguishable from other *Paranthaclisis* species by the following combination of adult characters [alternate state(s) in square brackets]: (1) pronotum with pale markings as follows: three maculations in a triangular pattern - two anteroparasagittal and one sagittal - and two lateral stripes (fig. 3b), (2) mesoscutum and mesoscutellum with long black setae and long white setae [not white setae only] (fig. 3c), (3) mesoscutellar rim with sagittal, yellow stripe [not with stripe absent] (fig. 3c), (4) hind wing with presectoral spurious vein connecting at least two adjacent crossveins [not present as lateral crossvein expansions only] (fig. 4b), (5) male abdomen with eversible sacs present [not absent] in intertergal membrane between tergites 6 and 7 (fig. 3e), (6) abdominal tergites with pale transverse markings along posterior margins [not with markings absent], markings usually expanded anteriorly on tergites six and seven (fig. 3e), (7) male ectoproct with postventral lobe distinctly angled [not straight] in lateral view (fig. 3d), (8) dorsal ridge of mediuncus smooth [without teeth or furrow] (fig. 4c).

2.4.2 Description

2.4.2.1 General

Body length: 30 – 39 mm (mean = 33, n = 60); *forewing length*: 32 – 43 mm (mean = 36, n = 60); *hind wing length*: 30 – 40 mm (mean = 34, n = 60).

2.4.2.2 Head (fig. 3a)

Vertex markings: dark brown, with short dark brown setae and short white setae, posterior area of vertex with pale parasagittal spots; *ocular rim*: with very few (usually < 10) white setae, ocular rim setae length < length of the pedicle.

2.4.2.3 Thorax (fig. 3b, c)

Pronotum: lateral markings pale, either as a continuous stripe, or broken near furrow and forming 2-3 distinct maculations; a pair of pale anteroparasagittal maculations present, lying in line behind parasagittal spots of vertex, a single pale maculation (sometimes reduced) present medially, the three pronotal marks forming a triangular pattern; *mesoscutum*: bearing long black setae and long white setae; *mesocutellum*: dark gray with pale posterolateral maculations, mesoscutellar rim color variable, but always pale sagittally.

2.4.2.4 Wings (fig. 4a, b)

Forewing: wing cells mostly hyaline, but with dark brown margining adjacent to all darkly-colored vein segments; costal area predominantly uniareolate adjacent to pterostigma; presectoral area with (6) 7 (8) crossveins; *hind wing*: weakly emarginate where MP1 meets wing margin; presectoral area with (5) 6 (7) crossveins; presectoral spurious vein connecting 2-3 adjacent crossveins.

2.4.2.5 Legs

General: dorsal surface of all tibiae banded with alternating brown and pale regions; ventral faces of all leg segments pale; *tarsus*: basal and distal tarsomeres with some pale markings, others brown; distal tarsomere length ≤ combined length of basal four tarsomeres.

2.4.2.6 Abdomen (fig. 3e)

General: posterior margin of most tergites with a pale transverse band, usually expanded anteriorly on tergites 6 and 7; *male*: with eversible sacs situated dorsolaterally in intertergal membrane between tergites 6 and 7.

2.4.2.7 Male terminalia (fig. 3d)

Ectoproct: postventral lobe length 2 1/2 to 3 times width at midpoint, obtusely angled posteriorly near midpoint.

2.4.2.8 Male genitalia (figs. 4c-e)

Gonarcus: extragonarcus a transverse plate with a widely bifurcated posterior margin, posterior face of extragonopons proximal to mediuncus shallowly invaginated in lateral view; *mediuncus*: length about 2 times middle width, not extending past gonocoxite 9 hooks in lateral view, dorsomedial ridge smooth in proximal half, without teeth or furrow.

2.4.3 Distribution (fig. 2a)

Western United States (widespread, northern Washington east to Wyoming and south to southern California and western Texas); northwestern Mexico (Sonora and the Baja peninsula). Based on available locality data this is the most widely distributed species of *Paranthaclisis*. Because *P. congener* has been recorded from several northern counties in the U.S. state of Washington, it is possible (but unconfirmed) that its range could extend northward into southwestern British Columbia.

2.4.4 Adult activity period

1 April – 31 October. Most commonly collected from June – August. Adult collection records for *P. congener* are ca. two months earlier in the southern part of its range (Arizona, Baja peninsula, California, Sonora, Texas) than in northern states (Oregon, Washington).

2.4.5 Biology

The oviposition behavior of *P. congener* was observed by Stange & Miller (1985) near the city of Reno, Nevada, U.S.A. Eggs were shallowly buried at dusk. Females laid oblong eggs in batches of up to 20 at a time, after the posterior gonapophyses were used to evenly coat each individual egg with sand prior to deposition. Eggs hatched in ca. 24 days.

2.4.6 Immature stages

Not examined. *Paranthaclisis congener* larvae were included in a generic review of the Acanthaclisini by Stange & Miller (1985), but no morphological, biological or behavioral traits unique to the species were noted. Stange & Miller (2012) included *P. congener* in a key to *Paranthaclisis* species larvae. The larva of *P. congener* was characterized as follows: "mandible about 2.5 times longer than width posterior to tooth; dorsal surface [of mandible] without short peg-like setae but with some elongate setae near base; dorsal surface of head capsule usually with four pronounced dark brown spots".

2.4.7 Primary type

Not located, not examined. The original description of *P. congener* by Hagen (1861) was based on only female material with the following collecting information: "Pecos River, Western Texas, July (Capt. Pope)". It is unclear from the original publication, however, whether the description is based on one or multiple female specimens. Hagen (1887) later stated that (bracketed [ ] information added): "the types (now destroyed) were four females from Pecos River, Western Texas (now N. Mexico), collected in July on Capt. Pope's expedition; one specimen of the same lot is still present in Mr. Uhler's [Mr. Phillip Reese Uhler (1835-1913)] coll". These five specimens mentioned by Hagen are assumed here to constitute the original type series. A species catalog of the North American Neuroptera by Penny et al. (1997) cited a holotype female in the MCZ, giving the same collecting information provided by Hagen (1887): "USA,

Pecos River, Western Texas (now N. Mexico)". Stange (2004) also cites a holotype female as being housed in the MCZ, and indicates (with an exclamation mark) that he had personally examined the specimen. A loan of this specimen was requested from the MCZ, but no *P. congener* type material could be located in the MCZ (Philip Perkins pers. comm. 2012). Additionally, no records could be found of a holotype female of *P. congener* ever having been deposited in the MCZ collection. Other institutions known (Horn and Kahle 1934) to have received specimens from Mr. Phillip Uhler's collection, i.e., California Academy of Natural Sciences, San Francisco, CA, U.S.A. (CAS) and National Museum of Natural History, Washington DC, U.S.A. (USNM), were also contacted but no *P. congener* type material has been located. A neotype should be designated in the future if the original type material is not found (Norm Penny, Oliver Flint pers. comm. 2012).

The precise collecting date, and location of the type locality, of *P.congener* has been a matter of some speculation. In the original description of *P. congener* (as *Acanthaclisis congener*), Hagen (1861) provided the following information for the specimens in his possession: "Pecos River, Western Texas, July (Capt. Pope)". Hagen (1887) later indicated that the type locality was actually a site in New Mexico. The specimens were collected by Captain John Pope (or possibly another member of his party), a U.S. military officer, member of the Corps of the Topological Engineers, and veteran of the Mexican war (Morris 1997), during one of the several expeditions that he commanded to the Llano Estacado region of western Texas and southeastern New Mexico. Because the type material was collected in July, it is clear the material was not

collected on the first Pope expedition as part of the Pacific Railroad Survey, which lasted from February to April of 1854 (Pope 1854). Pope returned to the area to conduct drilling operations in search of artesian water sources between February of 1855 and August of 1858. During this time, he and his men collected various plant and animal specimens that were documented by Pope in a "Book of Descriptions", including a collection of insects taken by Edmond Downing. A conservative estimate for possible collection dates for the *P. congener* type material would therefore be July of 1855, 1856, 1857 or 1858. However, because the specimens listed in Pope's "Book of Descriptions" were all collected between July 1855 and July 1856, one of these two years is likely the year of collection of the *P. congener* type series. Unfortunately, after consulting several sources that document Pope's expeditions (Morris 1997, Pope 1854, Pope 1955) and reviewing extensive unpublished research on the subject compiled by Horace R. Burke (Professor Emeritus, Department of entomology, Texas A&M University), it has not been possible to determine with certainty in which state (New Mexico or Texas) type locality of *P. congener* lies. Pope and this team made several camps along the Pecos River within a few miles north and south of the Texas/New Mexico border (Morris 1997). Due to the close proximity of these camps to the border, and the imprecision of recorded collecting localities, it is not now possible to confidently know from which state the type specimens originated.

2.4.8 Material examined (780 specimens; 243 ♂, 537 ♀)

UNITED STATES OF AMERICA: *Arizona*: Cochise, Coconino, La Paz, Maricopa, Navajo, Pima, Yuma; *California*: Imperial, Inyo, Kern, Lassen, Los Angeles, Mono, Riverside, San Bernardino, San Diego; *Idaho* [**New State Record**]: Canyon, Owyhee; *Nevada*: Carson City, Churchill, Clark, Humboldt, Lander, Lincoln, Nye, Pershing, Storey, Washoe; *New Mexico*: Doña Ana; *Oregon*: Columbia, Harney, Lane, Morrow, Multnomah, Sherman, Umatilla, Union; *Texas*: Brewster, El Paso, Ward; *Utah*: Emery, Garfield, Grand, Juab, Kane, Salt Lake, San Juan, Uintah, Washington; *Washington*: Benton, Chelan, Douglas, Grant, Okanogan; *Wyoming* [**New State Record**]: Park or Teton ("Yellowstone Park"). MEXICO: *Baja California [Norte]:* Ensenada, Mexicali, Playas de Rosarito; *Baja California Sur*: Mulegé, Los Cabos, Loreto; *Sonora* [**New State Record**]: Puerto Peñasco.

2.4.9 Etymology

Unexplained in original description, probably from the Latin adjective *congener*, of the same kind, in reference to its similarity to other species then placed in the genus *Acanthaclisis*.

2.4.10 Comments

Material representing a red morph of *P. congener* from Utah and Arizona was examined during this study. These specimens were not found to be different from normally-colored representatives in any key morphological features, including male

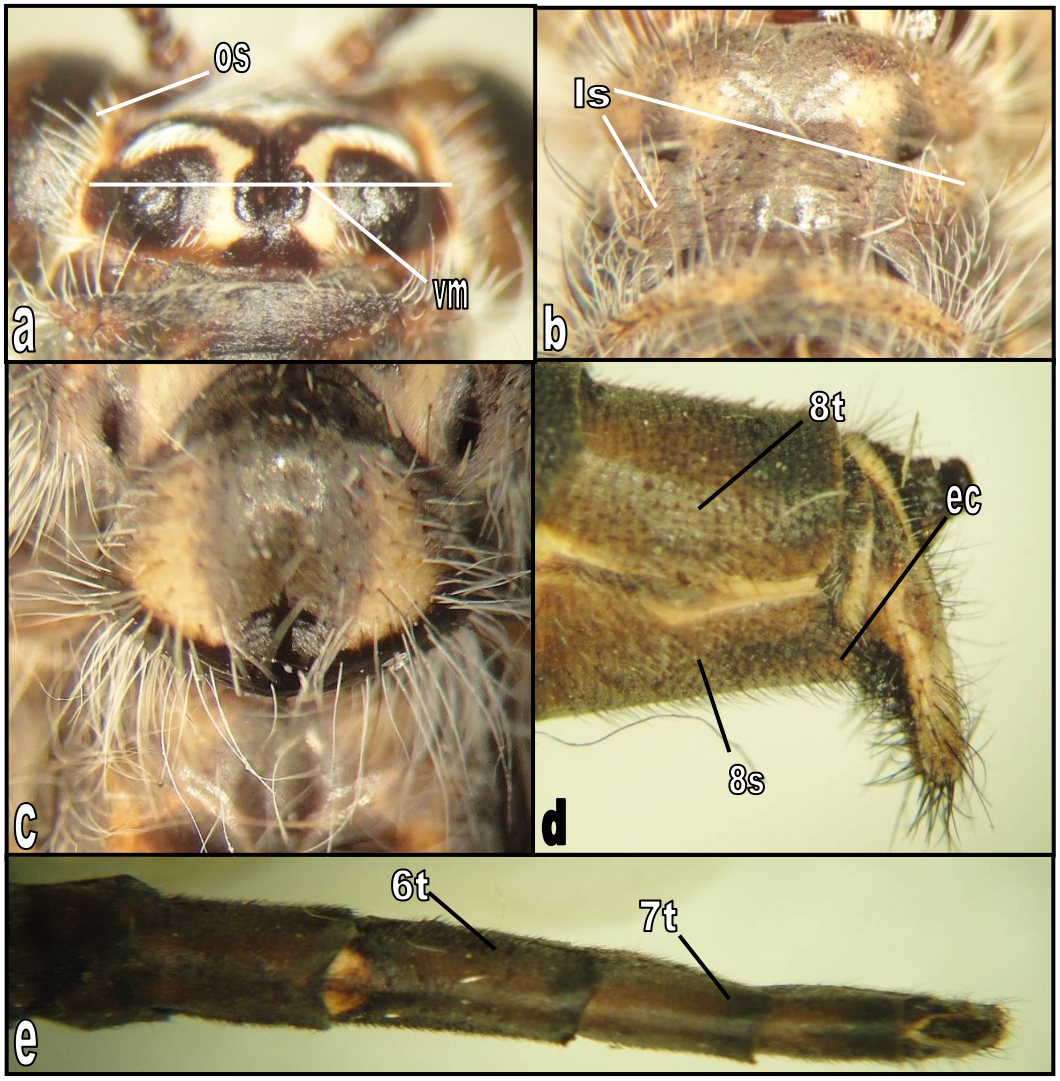

Fig. 5. *Paranthaclisis floridensis*, diagnostic characters. a, vertex, dorsal; b, pronotum, dorsal; c, mesothorax, dorsal; d, male abdomen, apex, lateral; e, male abdomen, dorsal. Abbreviations: 6t – 6th tergite; 7t – 7th tergite; 8s – 8th sternite; 8t – 8th tergite; ec – ectoproct; ls – lateral stripe; mr – mesoscutellar rim; os – ocular rim setae; vm – vertex markings.

genitalia. All red-morph material originated from several areas of northern Arizona and southern Utah that are known for red-colored rock formations. Perching substrate preferences for species of *Paranthaclisis* are largely unknown. However, individuals of *P. nevadensis* were observed by the author and John Oswald (Professor, Department of Entomology, Texas A&M University) resting on vegetation and the walls of a building adjacent to large sand dunes in southern California. Other myrmeleontid taxa have been reported to rest on vegetation (twigs and grasses), rock faces or the ground (Stange 1970). It is therefore possible that *P. congener* adults may rest on exposed rocks, cliff faces or the ground during the day, where a red color matching the surrounding substrate would aid in camouflaging an individual against potential predators. Similar protective color variation was discussed by Stange (1970) in connection with the widely distributed antlion species *Brachynemurus sackeni* (Myrmeleontinae: Brachynemurini). Unlike other *Brachynemurus* species, which are commonly found resting on vegetation, individuals of this species were observed to rest on rocks or the ground. Populations of *B. sackeni* found in habitats characterized by red sandstone displayed a pinkish hue, in contrast to more darkly colored specimens from other areas.

2.5 *Paranthaclisis floridensis* Stange & Miller (Figs. 2b, 5a-e, 6a-e)

Paranthaclisis floridensis Stange and Miller, 2012:1 (DN, FG- adult: abdomen (dorsal), head and pronotum (dorsal), habitus (dorsal and lateral); larva: habitus (dorsal and ventral), KA, KL, LA, OD, TA, TY). – Hagen 1887:151 (LA);

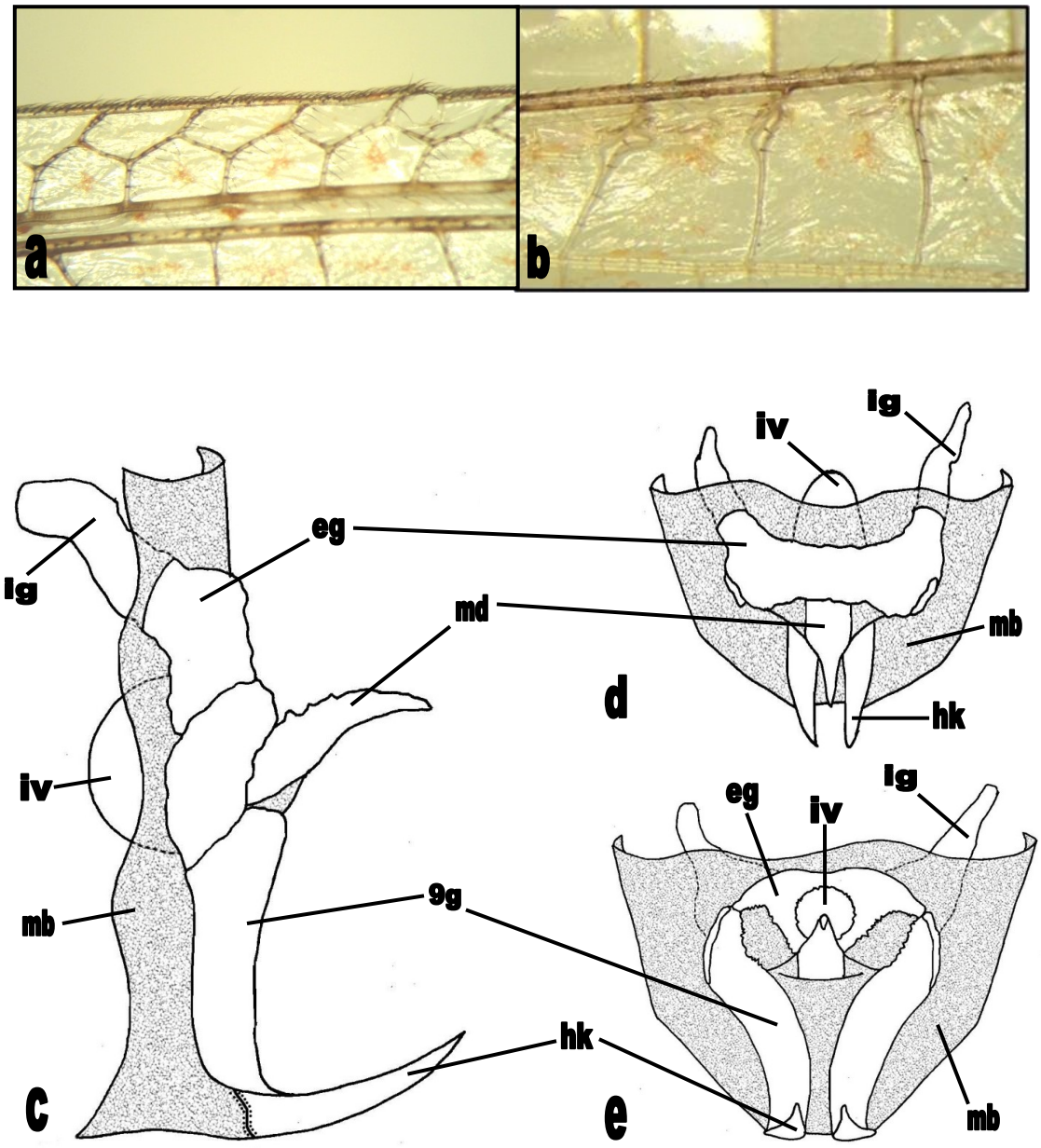

Fig. 6. *Paranthaclisis floridensis*, wings and male genitalia. a, forewing, costal area, dorsal; b, hind wing, presectoral area, dorsal; c, gonarcus complex, lateral; d, gonarcus complex, dorsal; e, gonarcus complex, posterior. Abbreviations: 9g – 9th gonocoxite; ex – extragonarcus; hk – apex of gonocoxite 9; ig – intragonarcus; iv – invagination of extragonopons; mb – membrane; md – mediuncus.

Stange 1970:21 (LA); Stange & Miller 1985: 32, 37 (DN, FG- larva: habitus (dorsal)); Stange 2004:356 (LS).

2.5.1 Diagnosis

Distinguishable from other *Paranthaclisis* species by the following combination of adult characters [alternate state(s) in square brackets]: (1) mesoscutum and mesoscutellum with long white and long black setae [with white setae only] (fig. 5c), (2) mesoscutellar rim lacking pale sagittal stripe [stripe present] (fig. 5c), (3) hind wing with presectoral spurious vein indicated only as expansions on lateral margins of presectoral crossveins [spurious vein connecting 2+ presectoral crossveins] (fig. 6b), (4) male abdomen with eversible sacs present [sacs absent] in intertergal membrane between tergites 6 and 7, (5) abdominal tergites entirely dark gray [tergites with pale markings on posterior margins] (fig. 5e), (6) male ectoproct with postventral lobe straight [lobe distinctly angled] in lateral view (fig. 5d), (7) dorsosagittal ridge of mediuncus with one row of teeth in proximal half [teeth absent] (fig. 6a), (8) forewing costal area partially biareolate in distal 1/3 [predominantly uniareolate in this region].

2.5.2 Description

2.5.2.1 General

Body length: 27 mm (n = 1); *forewing length*: 32 mm (n = 1); *hind wing length*: 29 mm (n = 1).

2.5.2.2 Head (fig. 5a)

Vertex markings: black, glabrous; *ocular rim*: with several (usually < 20 setae) white setae, running in a broken band from posterior margin of vertex markings to antenna, ocular rim setae length > length of the pedicle.

2.5.2.3 Thorax (figs. 5b, c)

Pronotum: lateral pale markings present, either as a continuous stripe, or broken near furrow and forming 2-3 distinct maculations, a pair of pale parasagittal stripes present (often reduced to a pair of anterior parasagittal maculations); *mesoscutum*: bearing long black and long white setae; *mesoscutellum*: anterior half dark gray, posterior half pale; mesoscutellar rim black, without pale sagittal stripe.

2.5.2.4 Wings (fig. 6a, b)

Forewing: coloration: wing cells hyaline, but with dark brown margining adjacent to darkly-colored longitudinal vein segments, most noticeable within mediocubital area; venation: costal area predominantly uniareolate adjacent to pterostigma; presectoral area with (6) 7 (8) crossveins; *hind wing*: venation: presectoral area with 5 (6) crossveins; presectoral spurious vein not connecting any presectoral crossveins, present only as lateral expansions on presectoral crossveins.

2.5.2.5 Legs

General: dorsal surface of all tibiae banded with alternating brown and pale regions; ventral faces of all leg segments brown; *tarsus*: all tarsomeres black; distal tarsomere length > combined length of four basal tarsomeres.

2.5.2.6 Abdomen (fig. 5e)

General: tergites entirely dark gray, posterior margins without pale transverse band(s); *male*: eversible sacs present dorsolaterally in intertergal membrane between tergites 6 and 7.

2.5.2.7 Male terminalia (fig. 5d)

Ectoproct: postventral lobe length about 3 1/2 times width at midpoint, directed ventrally, not angled near midpoint.

2.5.2.8 Male genitalia (figs. 6c-e)

Gonarcus: extragonarcus a transverse plate with a widely bifurcated posterior margin, posterior face of extragonarcus proximal to mediuncus deeply invaginated in lateral view; *mediuncus*: length 3 times middle width, extending past gonocoxite 9 hooks in lateral view; in dorsal view, basal half broad, subparallel sided, apical half attenuate, dorsomedial ridge with one row of teeth in proximal half.

2.5.3 Distribution (fig. 2b)

Eastern United States of America (Gulf and Atlantic coasts of northern Florida).

2.5.4 Adult activity period

May – 30 July.

2.5.5 Biology

Adults are active at night and can be collected using a light sheet.

2.5.6 Immature stages

Not examined. *Paranthaclisis floridensis* larvae were included in a generic review of the Acanthaclisini by Stange & Miller (1985), but morphological, biological and behavioral traits unique to this species were not addressed. Stange & Miller (2012) included *P. floridensis* in a key to the genus based on larval morphology. The following characters were used to distinguish the larvae of *P. floridensis* from *P. congener*, *P. hageni* and *P. nevadensis*: "mandible about 3.5 times longer than width posterior to tooth; dorsal surface [of mandible] with many peg-like setae; dorsal surface [of head capsule] at most with double dark brown spot near middle; abdomen with distinct longitudinal rows of dark brown markings; metathoracic setose tubercle with dark brown coloring; mandible with more than 20 peg-like setae distributed extending distad to mandibular tooth".

2.5.7 Primary type

Holotype ♂ (FSCA), not examined. Type locality: UNITED STATES OF AMERICA: *Florida*: Bay County: St. Andrews State Park.

2.5.8 Material examined (1 specimens; 1 ♂)

UNITED STATES OF AMERICA: *Florida*: Gulf.

2.5.9 Etymology

Unexplained in original description, probably Florid- [from the state of Florida] + -ensis [from Latin –*ensis*, belonging to], in reference to the type locality.

2.5.10 Comments

Only six adult specimens of *P. floridensis* are currently known (2 ♂, 2 ♀, FSCA; 1 ♂, TAMU; 1 ♂, USNM). Only one male specimen collected by the author was available during this study and therefore potential variation in morphological characters could not be thoroughly assessed. Descriptions and figures for this species are based on this male housed in the TAMU, as well as five specimens examined and photographed during a trip by the author to the FSCA in 2011. This species was recently described by Stange & Miller (2012) and is similar morphologically to *P. hageni* (see diagnosis). This species is treated as valid here, due to several diagnostic morphological characters, in the adults and larvae, and because of its current allopatric distribution in relation to other *Paranthaclisis* species. Stange & Miller (2012) suggest that if additional populations of

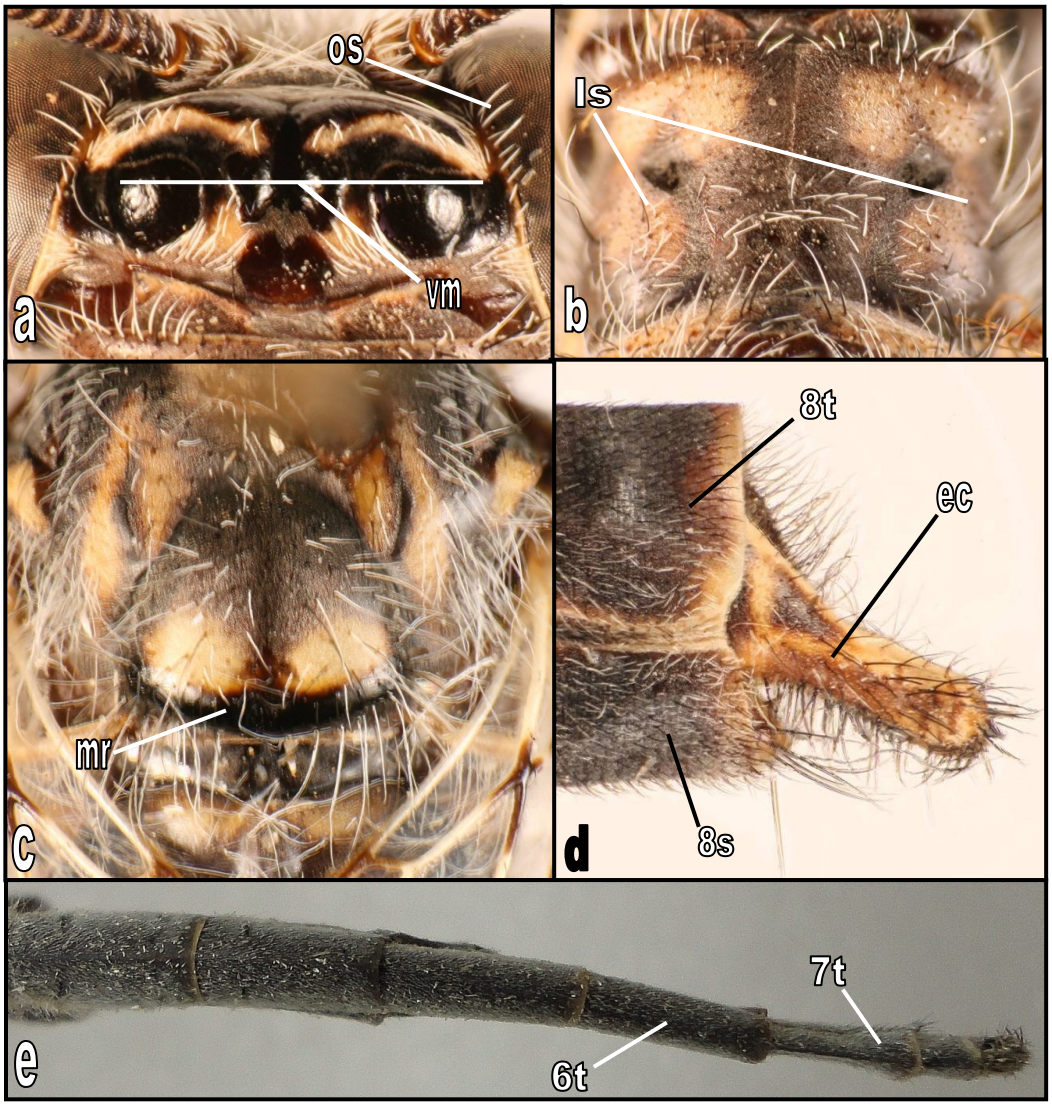

Fig. 7. *Paranthaclisis hageni*, diagnostic characters. a, vertex, dorsal; b, pronotum, dorsal; c, mesothorax, dorsal; d, male abdomen, apex, lateral; e, male abdomen, dorsal. Abbreviations: 6t – 6th tergite; 7t – 7th tergite; 8s – 8th sternite; 8t – 8th tergite; ec – ectoproct; ls – lateral stripe; mr – mesoscutellar rim; os – ocular rim setae; vm – vertex markings.

Paranthaclisis can be found along the Gulf Coast of the United States of America, linking *P. floridensis* to populations of *P.hageni*, *floridensis* could only represent geographic race of *hageni*. In order to investigate the validity of *P. floridensis*, additional specimens are needed to examine variation in key morphological characters, such as male genitalia and the partially biareolate costal area of the forewing, and the costal dune habitats of the Gulf Coast from Texas to Florida need to be sampled for potential *Paranthaclisis* populations.

2.6 *Paranthaclisis hageni* (Banks) (Figs. 2c, 7a-e, 8a-e)

Acanthaclisis hageni Banks, 1899:170 (OD); Currie 1903:274 (DN); Banks 1904:104 (LS).

Paranthaclisis hageni (Banks): Banks 1907a:275 (NO, TA); Banks 1907b:29 (LS); Banks 1911:71 (DN); Banks 1927:80-81 (DN, KA, RD); Banks 1939:4-5 (KA, TA); Banks 1942:148 (DN, LS); Stroud 1950:666 (LS); Stange 1961:674 (TY); Stange and Miller 1985:36-38, 40 (FG- larva head (dorsal and ventral), LA); Penny et al. 1997:75 (DN, LS, TY); Oswald et al. 2002:580 (LS); Clinebell et al. 2004:379, 389, 396-397 (FB, LS); Stange 2004:356 (DN, TA, TY); Gepp 2010: 34 (FG- adult habitus); Stange and Miller 2012:2-5 (KA, KL, LA).

Paranthaclisis californica Navás, 1920:189 (OD); Banks 1942:35 (NO, TA) (after Stange 2004).

Paranthaclisis californica Navás, 1922:390 (OD); Banks 1942:35 (NO, TA); Penny 1977:47 (DN, LS) **syn. n**.

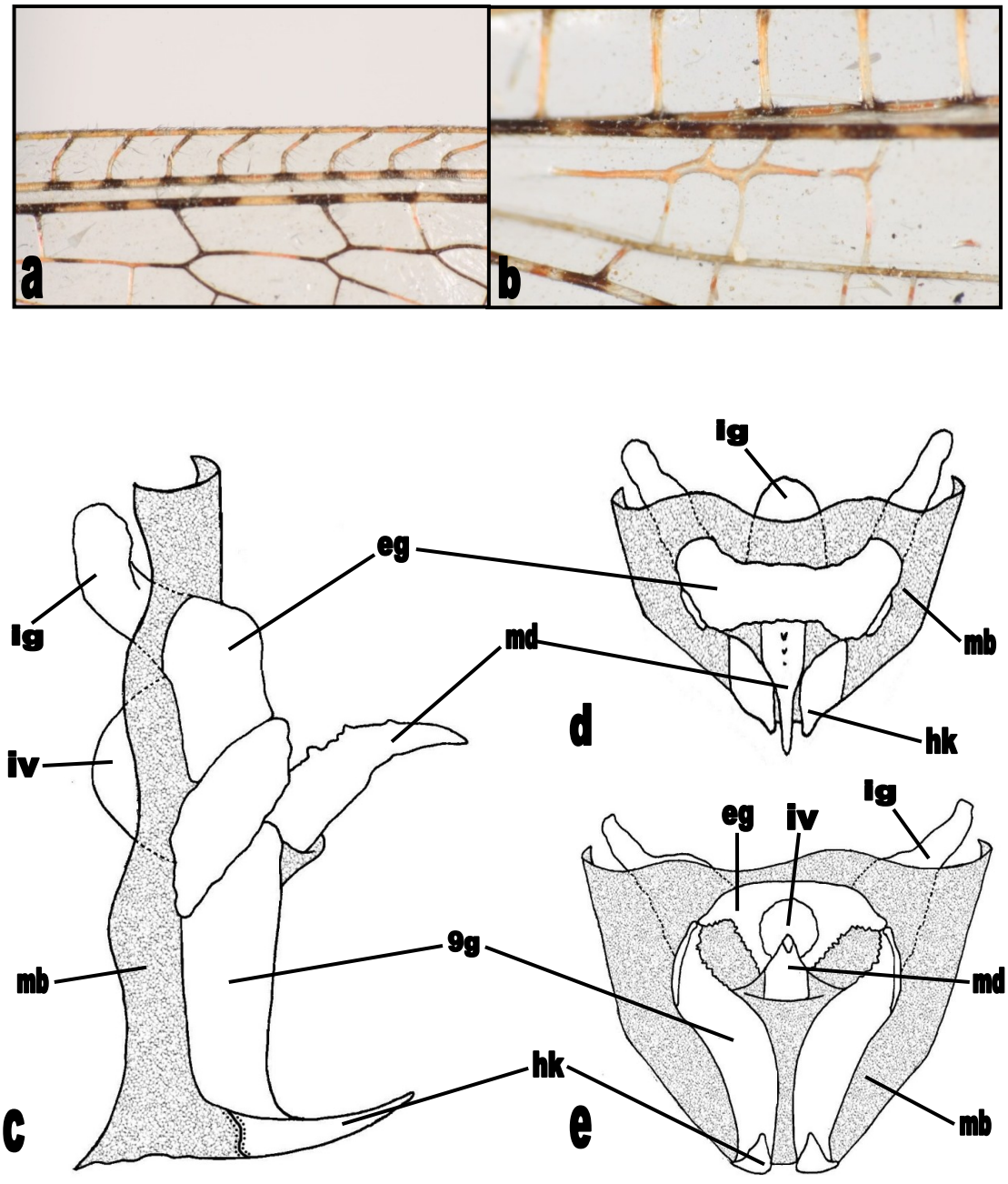

Fig. 8. *Paranthaclisis hageni*, wings and male genitalia. a, forewing, costal area, dorsal; b, hind wing, presectoral area, dorsal; c, gonarcus complex, lateral; d, gonarcus complex, dorsal; e, gonarcus complex, posterior. Abbreviations: 9g – 9th gonocoxite; ex – extragonarcus; hk – apex of gonocoxite 9; ig – intragonarcus; iv – invagination of extragonopons; mb – membrane; md – mediuncus.

2.6.1 Diagnosis

Distinguishable from other *Paranthaclisis* species by the following combination of adult characters [alternate state(s) in square brackets]: (1) mesoscutum and mesoscutellum with long white setae and long black setae [not with white setae only] (fig. 7c), (2) mesoscutellar rim lacking pale sagittal stripe [not present] (fig. 7c), (3) hind wing with presectoral spurious vein connecting at least two adjacent crossveins [not present as lateral expansions] (fig. 8b), (4) male abdomen with eversible sacs present [not absent] in intertergal membrane between tergites 6 and 7, (5) abdominal tergites entirely dark gray [not with pale transverse markings along posterior margins] (fig. 7e), (6) male ectoproct with postventral lobe straight [not distinctly angled] in lateral view (fig. 7d), (7) dorsal ridge of mediuncus with single row of teeth in proximal half [not smooth or with furrow] (fig. 8a).

2.6.2 Description

2.6.2.1 General

Body length: 26 – 35 mm (mean = 31, n = 60); *forewing length*: 31 – 37 mm (mean = 35, n = 60); *hind wing length*: 28 – 35 mm (mean = 33, n = 60).

2.6.2.2 Head (fig. 7a)

Vertex markings: black, glabrous; *ocular rim*: with several white setae, running in a broken band from posterior margin of vertex markings to antenna, usually < 20 setae, ocular rim setae length > length of the pedicle.

2.6.2.3 Thorax (figs. 7b, c)

Pronotum: lateral markings pale, a continuous stripe or broken at furrow or before, forming 2-3 maculations, a pair of pale parasagittal stripes (often reduced to only anterior maculations); *mesoscutum*: bearing long black setae and long white setae; *mesoscutellum*: anterior half dark gray, posterior half pale; mesoscutellar rim black, without pale sagittal marking.

2.6.2.4 Wings (fig. 8a, b)

Forewing: wing cells hyaline, but with dark brown margining adjacent to darkly-colored longitudinal vein segments, most noticeable within mediocubital area; predominantly uniareolate adjacent to pterostigma; presectoral area with 6-8 crossveins (usually 7); *hind wing*: area with 5-6 crossveins (usually 6); presectoral spurious vein connecting 2-3 adjacent crossveins.

2.6.2.5 Legs

General: dorsal surface of all tibias banded with alternating brown and pale regions; ventral faces of all leg segments brown; *tarsus*: all tarsomeres black; distal tarsomere > length of first four tarsomeres.

2.6.2.6 Abdomen (fig. 7e)

General: tergites entirely dark gray, posterior margins without a pale transverse band(s); *male*: with eversible sacs situated dorsolaterally in intertergal membrane between tergites 6 and 7.

2.6.2.7 Male terminalia (fig. 7d)

Ectoproct: postventral lobe length about 3 1/2 times width at midpoint, directed ventrally without angle near midpoint.

2.6.2.8 Male genitalia (figs. 8c-e)

Gonarcus: extragonarcus a transverse plate with a widely bifurcated posterior margin, posterior face of extragonarcus proximal to mediuncus deeply invaginated in lateral view; *mediuncus*: length 3 times middle width, extending past gonocoxite 9 hooks when viewed laterally; in dorsal view, basal half broad, subparallel sided, apical half attenuate, dorsomedial ridge with single row of teeth in proximal half.

2.6.3 Distribution (fig. 2c)

Southwestern United States (widespread, southern California east to central Texas and south to extreme southern Texas); northwestern Mexico (Chihuahua, Sonora and the Baja peninsula).

2.6.4 Adult activity period

29 April – 22 November. Most commonly collected from June – August.

2.6.5 Biology

Adults of *Paranthaclisis hageni* were observed by Clinebell et al. (2004) foraging for nectar on *Gaura* (Onagraceae: Onagreae) flowers in the Permian Basin region of western Texas. Pollen loads on the external body surfaces of *hageni* individuals collected during the study ranged from 0 to 500 grains. A related antlion species, *Vella fallax* (Myrmeleontidae: Acanthaclisini), was also observed visiting *Gaura* flowers, although the authors suggest this species may have been feeding on moths, rather than pollen or nectar, due to the presence of scales covering the body.

2.6.6 Immature stages

Not examined. *Paranthaclisis hageni* larvae were included in a generic review of the Acanthaclisini by Stange & Miller (1985), but morphological, biological and behavioral traits unique to this species were not addressed. Stange & Miller (2012) included *P. hageni* in a key to the genus based on larval morphology. Stange & Miller were not able to distinguish between larval specimens of *P. hageni* and *P. nevadensis* and these two species were treated as one unit in the key provided. The following characters were used to distinguish the larvae of *P. hageni* from *P. congener* and *P. floridensis*: "mandible about 3.5 times longer than width posterior to tooth; dorsal

surface [of mandible] with many peg-like setae; dorsal surface [of head capsule] at most with double dark brown spot near middle; abdomen unmarked; metathoracic setose tubercle all pale brown; mandible with less than 10 peg-like setae distributed basad to mandibular tooth".

2.6.7 Primary type

Lectotype ♂ (MCZ; type # 10592, designated by Stange, 1961), not examined. Type locality: UNITED STATES OF AMERICA: *Arizona*, Phoenix.

2.6.8 Material examined (636 specimens; 206 ♂, 430 ♀)

UNITED STATES OF AMERICA: *Arizona*: Cochise, Graham, La Paz, Maricopa, Pima, Pinal, Yuma; *California*: Imperial, Inyo, Riverside, San Bernardino, San Diego; *Nevada*: Nye; *New Mexico*: Bernalillo, Chaves, Dona Ana, Eddy, Hidalgo, Lea, Luna, Otero, Socorro; *Texas*: Brewster, Cameron, Cottle, Culberson, El Paso, Hemphill, Hudspeth, Jeff Davis, Kenedy, Nueces, Presidio, Reeves, Ward, Wichita, Wilson, Winkler. *MEXICO*: *Baja California [Norte]:* Mexicali; *Baja California Sur*: Comondu, Mulegé, La Paz, Los Cabos, Loreto; *Chihuahua* [**New State Record**]: Julimes*; Sonora*: Puerto Peñasco.

2.6.9 Etymology

Unexplained in original description, probably from the surname of German/American entomologist Herman August Hagen (1817-1893).

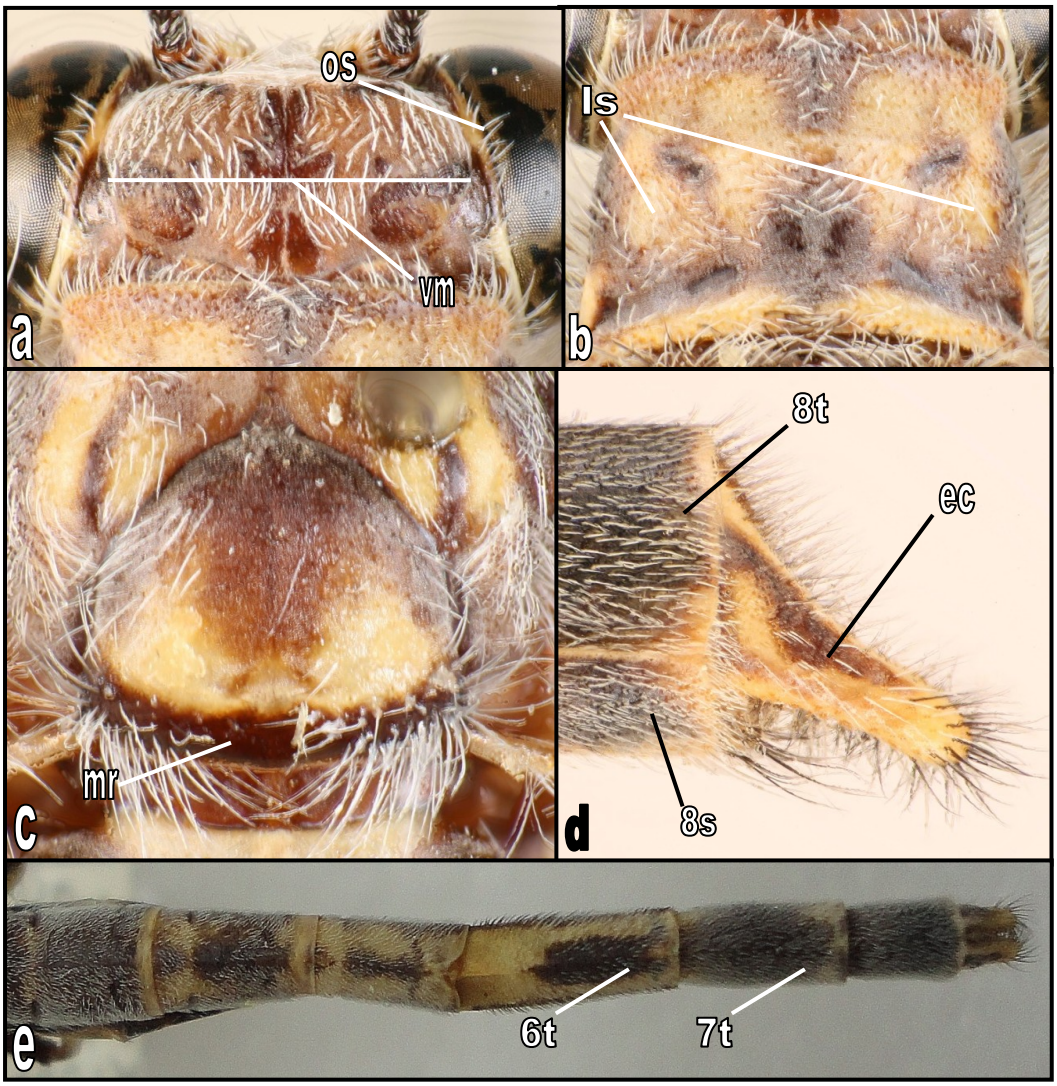

Fig. 9. *Paranthaclisis nevadensis*, diagnostic characters. a, vertex, dorsal; b, pronotum, dorsal; c, mesothorax, dorsal; d, male abdomen, apex, lateral; e, male abdomen, dorsal. Abbreviations: 6t – 6th tergite; 7t – 7th tergite; 8s – 8th sternite; 8t – 8th tergite; ec – ectoproct; ls – lateral stripe; mr – mesoscutellar rim; os – ocular rim setae; tb – transverse band; vm – vertex markings.

2.7 *Paranthaclisis nevadensis* Banks (Figs. 2d, 9a-e, 10a-e)

Paranthaclisis nevadensis Banks, 1939:4 (FG- adult male terminalia, KA, MT, OD); Penny et al. 1997:75 (DN, LS, TY); Stange 2004:356 (DN, TA, TY); Stange & Miller 1985:37 (LA); Stange & Miller 2012:1-3, 5 (KA, KL, LA).

2.7.1 Diagnosis

Distinguishable from other *Paranthaclisis* species by the following combination of adult characters [alternate state(s) in square brackets]: (1) mesoscutum and mesoscutellum with long white setae only [with black and white setae] (fig. 9c), (2) mesoscutellar rim lacking pale sagittal stripe [stripe present] (fig. 9c), (3) hind wing with presectoral spurious vein indicated only as expansions on lateral margins of presectoral crossveins [spurious vein connecting 2+ presectoral crossveins] (fig. 10b), (4) male abdomen without eversible sacs [sacs present] in intertergal membrane between tergites 6 and 7, (5) abdominal tergites with pale transverse markings on posterior margins [not with markings absent], markings usually expanded anteriorly on tergites 4, 5 and 6 (fig. 9e), (6) male ectoproct with postventral lobe straight [lobe distinctly angled] in lateral view (fig. 9d), (7) dorsosagittal ridge of mediuncus with furrow in proximal half [furrow absent] (fig. 10a).

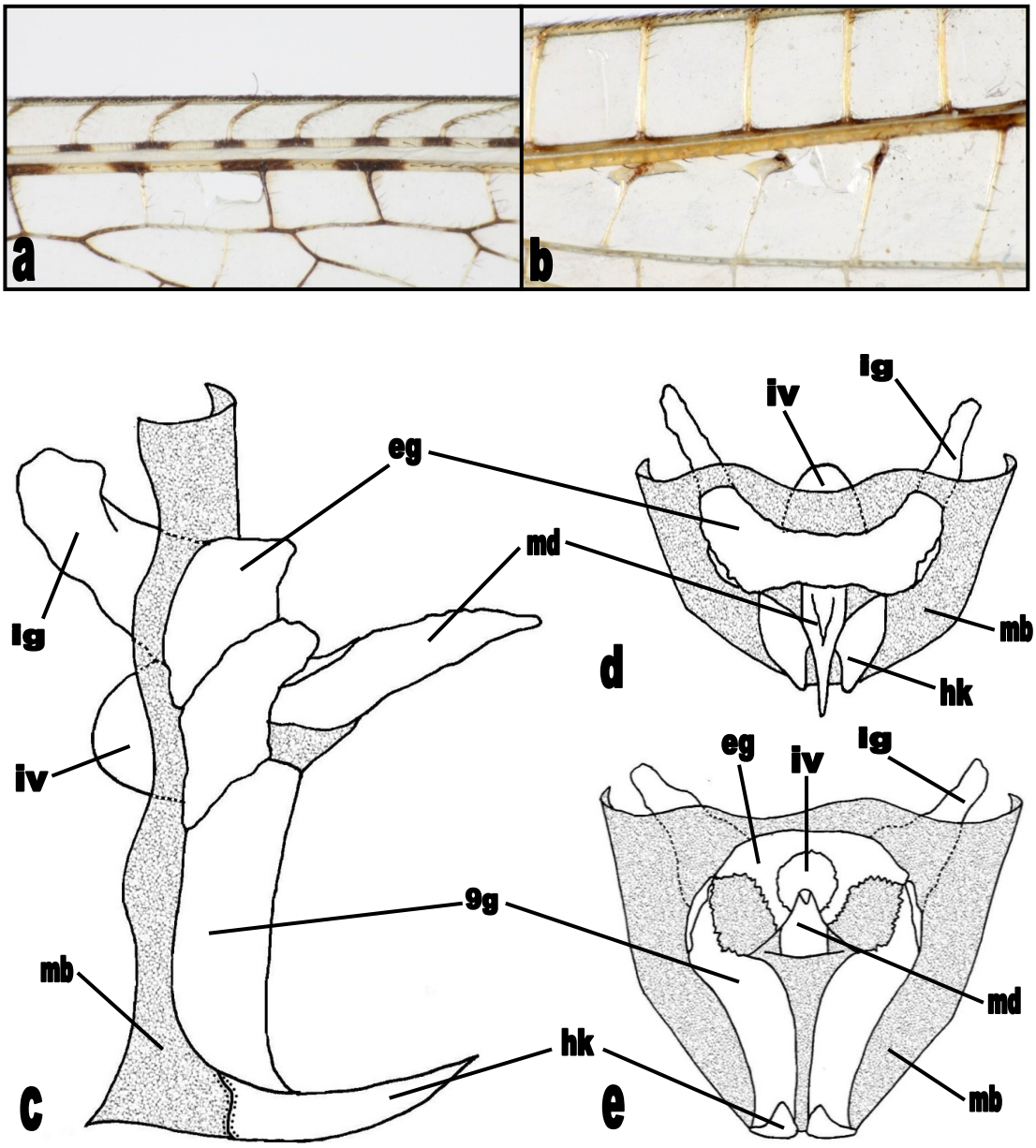

Fig. 10. *Paranthaclisis nevadensis*, wings and male genitalia. a, forewing, costal area, dorsal; b, hind wing, presectoral area, dorsal; c, gonarcus complex, lateral; d, gonarcus complex, dorsal; e, gonarcus complex, posterior. Abbreviations: 9g – 9th gonocoxite; ex – extragonarcus; hk – apex of gonocoxite 9; ig – intragonarcus; iv – invagination of extragonopons; mb – membrane; md – mediuncus.

2.7.2 Description

2.7.2.1 General

Body length: 28 – 36 mm (mean = 31, n = 60); *forewing length*: 29 – 36 mm (mean = 32, n = 60); *hind wing length*: 27 – 33 mm (mean = 30, n = 60).

2.7.2.2 Head (fig. 9a)

Vertex markings: dark brown, with short white setae; *ocular rim*: with many (usually > 30 setae) white setae, running in a continuous band from posterior margin of vertex markings to antenna, ocular rim setae length > length of the pedicle.

2.7.2.3 Thorax (figs. 9b, c)

Pronotum: lateral markings pale, either as a continuous stripe, or broken near furrow and forming 2-3 distinct maculations; a pair of pale parasagittal stripes (often joined medially); *mesoscutum*: bearing long white setae only; *mesoscutellum*: anterior half dark gray, posterior half pale; mesoscutellar rim dark brown, without pale sagittal marking.

2.7.2.4 Wings (fig. 10a, b)

Forewing: coloration: wing cells hyaline, but with dark brown margining adjacent to darkly-colored longitudinal vein segments, most noticeable within mediocubital area; venation: costal area predominantly uniareolate adjacent to pterostigma; presectoral area with (6) 7 (8) crossvein; *hind wing*: venation: presectoral

area with 5 (6) crossveins; presectoral spurious vein not connecting any presectoral crossveins, present only as lateral expansions on presectoral crossveins.

2.7.2.5 Legs

General: dorsal surface of all tibiae banded with alternating brown and pale regions; ventral faces of all leg segments brown; *tarsus*: all tarsomeres black; distal tarsomere length > combined length of four basal tarsomeres.

2.7.2.6 Abdomen (fig. 9e)

General: posterior margin of most tergites with a pale transverse band, usually expanded anteriorly on tergites 4, 5 and 6; *male*: eversible sacs absent.

2.7.2.7 Male terminalia (fig. 9d)

Ectoproct: postventral lobe length about 2 times width at midpoint, directed ventrally, not angled near midpoint.

2.7.2.8 Male genitalia (figs. 10c-e)

Gonarcus: extragonarcus a transverse plate with a widely bifurcated posterior margin, posterior face of extragonarcus proximal to mediuncus deeply invaginated in lateral view; *mediuncus*: length 3 1/2 times middle width, extending past gonocoxite 9 hooks in lateral view; in dorsal view, basal half broad, subparallel sided, apical half attenuate, dorsomedial ridge with longitudinal furrow in proximal half.

2.7.3 Distribution (fig. 2d)

Southwestern United States of America (western Nevada south to southern California and western Arizona; northwestern Mexico (Sinaloa and Sonora).

2.7.4 Adult activity period

4 May – 26 September.

2.7.5 Biology

Adults were collected in southern California (Imperial County) by the author and John Oswald on August 12th, 2010. Individuals were observed resting on vegetation and on the walls of a building during the early afternoon. Because this species has been frequently collected using light traps, it is likely these *P. nevadensis* adults had been attracted to the lights of the building the night before and had yet to leave the area. Several individuals flew from the building to nearby plants when disturbed.

2.7.6 Immature stages

Not examined. *Paranthaclisis nevadensis* larvae were included in a generic review of the Acanthaclisini by Stange & Miller (1985), but morphological, biological and behavioral traits unique to this species were not addressed. Stange & Miller (2012) included *P. nevadensis* in a key to the genus based on larval morphology. Stange & Miller were not able to distinguish between larval specimens of *P. nevadensis* and *P.*

hageni and these two species were treated as one unit in the key. The following characters were used to distinguish the larvae of *P. nevadensis* from *P. congener* and *P. floridensis*: "mandible about 3.5 times longer than width posterior to tooth; dorsal surface [of mandible] with many peg-like setae; dorsal surface [of head capsule] at most with double dark brown spot near middle; abdomen unmarked; metathoracic setose tubercle all pale brown; mandible with less than 10 peg-like setae distributed basad to mandibular tooth".

2.7.7 Primary type

Holotype ♂ (ANSP; type # 9103), not examined. Type locality: UNITED STATES OF AMERICA: *Nevada*: Esmeralda County: Clayton Valley, 2 mi S Silver Peak.

2.7.8 Material examined (181 specimens; 65 ♂, 116 ♀)

UNITED STATES OF AMERICA: *California*: Imperial, Inyo, Kern, Los Angeles, Riverside, San Bernardino; *Nevada*: Churchill, Esmeralda, Nye; *MEXICO* [**New Country Record**]: *Sinaloa*: Ahome; *Sonora*: Puerto Peñasco.

2.7.9 Etymology

Unexplained in original description, probably Nevad- [from the state of Nevada] + -ensis [from Latin –*ensis*, belonging to], in reference to the type locality.

2.8 Key to Adult *Paranthaclisis*

Note: The key below is for adult males and adult females. For a key to the larvae, see Stange & Miller 2012.

1 Mesoscutellar rim dark sagitally (figs. 5c, 7c, 9c); basal and distal tarsomeres entirely black; male terminalia: ectoproct of postventral lobe not obtusely angled near midpoint in lateral view (figs. 5d, 7d, 9d); male genitalia: extragonarcus with posterior face deeply invaginated proximal to mediuncus (invagination ≥ 2/3 mediuncus length) (figs. 6e, 8e, 10e)…….……...…….…..2

1' Mesoscutellar rim pale sagittally (fig. 3c); basal and distal tarsomeres brown, with some pale markings; male terminalia: postventral lobe of ectoproct obtusely angled near midpoint in lateral view (fig. 3d); male genitalia: extragonarcus with posterior face shallowly invaginated proximal to mediuncus (invagination < 1/3 mediuncus length) (fig. 4e)……..….*Paranthaclisis congener*

2(1) Head: vertex markings black, shining, asetose (figs. 5a, 7a); abdomen: tergites without transverse pale markings on posterior margins (figs. 5e, 7e); male genitalia: mediuncus proximally with a dorsosagittal ridge consisting of a single row of teeth (figs. 6c, 8c)…….……...…...3

2' Head: vertex markings dark brown, not shining, setose (fig. 9a); abdomen: tergites with pale transverse markings on posterior margin (expanded on tergites 4 – 6; fig. 9e); male genitalia: mediuncus proximally with a dorsosagittal furrow, teeth absent (fig. 10c)……..……...……..*Paranthaclisis nevadensis*

3(2) Forewing: costal area uniareolate throughout (fig. 8a); hind wing: presectoral spurious vein connecting at least two presectoral crossveins (fig. 8b); ……..... *Paranthaclisis hageni*

3' Forewing: costal area uniareolate proximally, biareolate distally near pterostigma (fig. 6a); hind wing: presectoral spurious vein indicated only as expansions on lateral margins of presectoral crossveins, not connecting any presectoral crossveins (fig. 6b).....*Paranthaclisis floridensis*

2.9 Future Research

Potential areas for additional research in *Paranthaclisis* include the following: (1) collecting along the Gulf Coast of the southern United States of America. The description of *P. floridensis* in Florida by Stange and Miller (2012) represents a major range extension for the genus (previously recorded only as far east as Texas) and the potential of undiscovered *Paranthaclisis* populations existing in the coastal dunes between Texas and the Florida should be investigated. (2) behavioral studies of adults and larvae. Little behavioral information is available for adult *Paranthaclisis*. Additional observations could be made in the field or laboratory to investigate the feeding, mating and perching strategies for these insects. Larval behavior was previously discussed by Stange & Miller (1985). Future studies on *Paranthaclisis* larvae may focus on prey choice, microhabitat preferences or natural predators and parasites. (3) maintenance of species boundaries where two or more species are sympatric. Based on available locality

data, there are several areas in the southwestern United States of America and northwestern Mexico in which two or three *Paranthaclisis* can be collected. Potential factors contributing to conservation of species limits that could be investigated include spatial or temporal niche partitioning and morphological variation. Bruce Miller (pers. comm.) suggested that larvae of *Paranthaclisis* species may prefer different types of substrate, including windblown or water deposited sand. It is also possible that adults of sympatric *Paranthaclisis* species display different activity periods, limiting interspecific mating opportunities. Morphological variation is evident in terminalic and genitalic structures of *Paranthaclisis* males and could contribute to the maintenance of species boundaries in the presence of multiple species. Population studies using molecular markers could be conducted to test for introgression between species.

3. PHYLOGENETIC ANALYSIS

3.1 Introduction

Few phylogenetic analyses have been conducted investigating the relationships of taxa within the family Myrmeleontidae, all of which have been based entirely on morphological characters. The tribe Palparini was analyzed by Mansell (1992) as part of a larger revisionary work and resulted in his division of the tribe into four genus groups. Stange (1994) provided the most comprehensive morphological analyses of the family to date, which included all three currently-recognized subfamilies and 12 of the 14 currently-recognized tribes. Most recently, a cladogram was constructed for the antlion fauna of Egypt (El-Hamoley *et al.* 2000), in which the authors classified the taxa of the region into three subfamilies and five tribes. Several investigations of the relationship among the holometabolous insect orders (Carmean et al. 1992, Whiting et al. 1997, Cameron et al. 2009), and within the superorder Neuropterida (Haring & Aspock 2004, Cameron et al. 2009, Winterton 2003, Winterton et al. 2010) have included molecular data for several gene regions for selected myrmeleontid taxa, but molecular data have yet to be used explicitly for phylogenetic analyses within the family Myrmeleontidae.

The goal of this study was to investigate the monophyly of *Paranthaclisis* and its phylogenetic relationships with other acanthaclisine genera, using selected taxa from another neuropteran family as a root outgroup. The monophyly of *Paranthaclisis* is informally supported by several morphological characters, but these characters have yet to be evaluated in a more rigorous phylogenetic framework. Phylogenetic analyses,

using both morphological and molecular (16S, 18S) characters, were conducted using several inference methods (maximum parsimony, maximum likelihood and Bayesian) and dataset treatments. The influences on topology and clade support for different sequence alignment programs, different data partitioning methods and different mixed dataset analysis techniques (morphology and molecular characters) were also investigated.

3.2 Materials and Methods

3.2.1 Taxon Selection

The four valid species in *Paranthaclisis* were considered to constitute the putative ingroup for phylogenetic analyses in this study: *P. congener* (Hagen), *P. floridensis* Stange & Miller, *P. hageni* (Banks), and *P. nevadensis* Banks. Six additional taxa were included as outgroups: *Vella fallax* (Rambur), *Heoclisis fundata* (Walker), *Cosina annulata* (Esben-Petersen), *Myrmeleon texanus* (Banks), *Myrmeleon mexicanus* (Banks), and *Nemoptera bipennis* (Illiger) (Table 1). *Vella fallax*, *H. fundata* and *C. annulata* were selected as additional representatives of the antlion tribe Acanthaclisini and were included to test the monophyly of *Paranthaclisis*, and to provide a preliminary framework of support for intergeneric relationships within this tribe. *Paranthaclisis* and *Vella* are the only two New World genera in the tribe Acanthaclisini. While the monophyly of *Paranthaclisis* + *Vella* might be assumed based on this current geographical distribution, there is evidence that supports the alternative hypothesis that the New and Old World Acanthaclisini do not constitute mutually exclusive

monophyletic groups. Stange & Miller (1985) suggested, based on adult and larval morphology, that *Paranthaclisis* (New World) may group phylogenetically with *Centroclisis* (Old World), and that *Vella* (New World) may group with *Heoclisis* (Old World). Representatives of the Old World genera *Heoclisis* and *Cosina* were included in the analysis to investigate these alternative hypotheses. *Myrmeleon texanus* and *M. mexicanus* belong to a different antlion tribe, the Myrmeleontini, and were included to test the monophyly of tribe Acanthaclisini. One representative of the closely-related family Nemopteridae, *N. bipennis* (Illiger), was included as a distant outgroup to root trees in all analyses. Previous phylogenetic research (Haring & Aspöck 2004, Winterton et al. 2010) has shown that the family Nemopteridae is the sister-group of the Myrmeleontidae + Ascalaphide. Although the Ascalaphidae (owlfiles) has often been assumed to constitute the sister-group of the Myrmeleontidae, the root outgroup chosen here was not selected from Ascalaphidae because recent morphological and molecular

Table 1. Selected ingoup and outgroup taxa included in all analyses.

Taxon	Order	Family	Tribe/Subfamily	Distribution
Paranthaclisis congener	Neuroptera	Myrmeleontidae	Acanthaclisini	New World
Paranthaclisis floridensis	Neuroptera	Myrmeleontidae	Acanthaclisini	New World
Paranthaclisis hageni	Neuroptera	Myrmeleontidae	Acanthaclisini	New World
Paranthaclisis nevdensis	Neuroptera	Myrmeleontidae	Acanthaclisini	New World
Vella fallax	Neuroptera	Myrmeleontidae	Acanthaclisini	New World
Heoclisis fundata	Neuroptera	Myrmeleontidae	Acanthaclisini	Old World
Cosina annulata	Neuroptera	Myrmeleontidae	Acanthaclisini	Old World
Myrmeleon texanus	Neuroptera	Myrmeleontidae	Myrmeleontini	New World
Myrmeleon mexicanus	Neuroptera	Myrmeleontidae	Myrmeleontini	New World
Nemoptera bipennis	Neuroptera	Nemopteridae	Nemopterinae	Old World

analyses have failed to demonstrate that both Ascalaphidae and Myrmeleontide are monophyletic (Winterton et al. 2010), casting doubt on their putative sister-group status.

3.2.2 Morphological Characters

Eighteen binary and multistate morphological characters were sampled from across adult body regions (Table 2). Characters were selected from those previously used in phylogenetic analyses within the Myrmeleontidae (Stange 1994) or were generated by the author by examining included taxa using a dissecting microscope. Missing data (characters 7 and 8) for the outgroup *Nemoptera bipennis* were scored as "?". These morphological characters were unable to be scored due the highly derived hindwing structure present in family Nemopteridae. All morphological characters were treated as unweighted and unordered in all phylogenetic analyses.

Table 2. Data matrix used for morphological phylogenetic analyses.

Taxon	Character Number																	
	0	0	0	0	0	0	0	0	0	0	1	1	1	1	1	1	1	1
	0	1	2	3	4	5	6	7	8	9	0	1	2	3	4	5	6	7
P. congener	1	2	1	1	0	1	1	2	1	1	0	1	1	1	3	1	1	1
P. floridensis	2	2	1	1	1	1	1	1	1	1	0	1	1	1	3	1	1	1
P. hageni	2	2	1	1	0	1	1	2	1	1	0	1	1	1	3	1	1	1
P. nevdensis	2	2	1	1	0	1	1	1	1	1	0	1	1	1	3	1	0	1
Vella fallax	1	2	1	1	1	1	1	0	2	1	0	2	2	1	2	1	1	2
Heoclisis fundata	1	2	1	1	2	1	1	2	2	1	0	1	2	1	1	2	1	1
Cosina annulata	1	1	1	1	2	1	1	0	2	1	0	1	1	0	2	1	1	2
M. texanus	0	1	1	1	0	1	1	0	0	1	0	1	1	0	1	0	0	0
M. mexicanus	0	1	1	1	0	1	1	0	0	1	0	1	1	0	1	0	0	0
Nemoptera bipennis	0	0	0	0	0	0	0	?	?	0	1	0	0	0	0	0	0	0

P. = Paranthaclisis; M. = Myrmeleon

Head:

Character 0: *Ocular rim setae*.

(0) absent [ancestral or lost];

(1) short;

(2) long.

Comments: Taxa coded as state (1) have ocular rim setae that are shorter than the length of the pedicle. Short ocular rim setae are sometimes difficult to observe because of their small size. In character state (2), the ocular rim setae are longer than the length of the pedicle.

Character 1: *Palpimacula pit of labial palp sensory area*.

(0) absent [ancestral or lost];

(1) oval shaped;

(2) slit shaped.

Character 2: *Antenna, shape*.

(0) filiform;

(1) clavate.

Comments: This character is taken from Stange (1994).

Thorax:

Character 3: *Pronotum, shape*.

(0) wider than long;

(1) as long as wide or longer.

Comments: In state (0), the width of the pronotum at its midpoint is greater than its length along the sagittal plane. In state (1), the width of the pronotum at its midpoint is less than its length along the sagittal plane. This character is taken from Stange (1994).

Wings:

Character 4: *Forewing, costal area*.

(0) predominantly uniareolate, before and after origin of Rs;

(1) partially biareolate, beginning after Rs origin;

(2) predominantly biareolate, before and after origin of Rs.

Comments: In state (0), there are usually no crossveins present in the costal area, resulting in undivided costal cells. In state (1), a series of costal cells distal to the origin of the radial sector is divided by a series of crossveins into upper and lower parts (the biareolate condition). In state (2), the majority of cells along the entire length of the costal area are divided into two parts by crossveins. The costal area, as defined by Stange (1970), is the space between the costa and subcosta, running from the base of the wing to the pterostigma. The costal area is divided into cells by short veinlets running from the subcosta to the costa (the uniareolate condition). The division of inter-veinlet costal area cells by one or more crossveins has been used for identification purposes within several groups within the Myrmeleontidae.

Character 5: *Forewing, origin of Rs*.

(0) in middle 1/3 of wing;

(1) in basal 1/3 of wing.

Character 6: *Forewing, hypostigmatic cell*.

(0) short;

(1) long.

Comments: In state (0), the hypostigmatic cell is less than three times longer than it is wide. In state (1), the hypostigmatic cell is more than 5 times longer than it is wide. All myrmeleontid taxa exhibit state (1), which is considered a snypomorphy of the family.

Character 7: *Hind wing, presectoral spurious vein*.

(0) absent [ancestral or lost];

(1) present, lateral expansions on crossveins only;

(2) present, connecting two or more presectoral crossveins.

Comments: For discussion of the presectoral spurious vein, see Materials and Methods, Terminology. In state (0) there is no indication of the presectoral spurious vein in the presectoral area of the hind wing. The presectoral spurious vein is present in state (1), but only indicated as lateral expansions on some presectoral crossveins in the presectoral area of the hind wing. In state (2), the presectoral spurious vein is present and connects two or more crossveins in the presectoral area of the hind wing.

Character 8: *Hind wing, CuA and MP2*.

(0) CuA and posterior fork of MP2 running free to wing margin;

(1) CuA and posterior fork of MP2 fuse before wing margin, approach asymmetrical;

(2) CuA and posterior fork of MP2 fuse before wing margin, approach symmetrical.

Comments: In state (0), the CuA and posterior fork of the MP_2 in the hind wing do not fuse, but may be joined by one or more crossveins. In state (1), the posterior fork of the MP_2 in the hind wing is united with the CuA after sharply bending toward the base of the wing (fig. 1a). This character shows some variation in *Paranthaclisis* in both the length of the MP_2 fork decurved veinlet and the angle at which the posterior fork of the MP_2 and CuA join. The posterior fork of the MP_2 and CuA also fuse in the hind wing in state (2), but after gradually converging over a short distance.

Character 9: *Hind wing, male, pilula axilaris*.

(0) absent [ancestral or lost];

(1) present.

Character 10: *Hind wing shape*.

(0) elongate, oval;

(1) remiform.

Comments: The highly elongate hind wing is apomorphic for the family Nemopteridae. This character is taken from Stange (1994).

Legs:

Character 11: *Proleg, femur, elongate sense hair(s)*.

(0) 0;

(1) 1;

(2) 2.

Character 12: *Mesoleg, femur, elongate sense hair(s)*.

(0) 0;

(1) 1;

(2) 2.

Character 13: *Metaleg, femur, elongate sense hair(s)*.

(0) 0;

(1) 1;

(2) 2.

Character 14: *Legs (all), tibial spurs*.

(0) absent [ancestral or lost];

(1) present, nearly straight;

(2) present,evenly curved, a near semi circular arch;

(3) present, bent at ca. 90˚ near midpoint.

Character 15: *Legs (all), pretarsal claws*.

(0) slightly curved;

(1) sharply bent near base.

Abdomen:

Character 16: *Tergites 6 & 7, male, intertergal membrane, eversible sacs*.

(0) absent [ancestral or lost];

(1) present.

Comments: For discussion of the male eversible sacs, see Materials and Methods, Terminology.

Male terminalia:

Character 17: *Ectoproct, postventral lobe*.

(0) absent;

(1) long;

(2) very long.

Comments: In state (0), the male ectoproct is lacking a postventral lobe. In state (1), the postventral lobe of the male ectoproct is less than or equal to 3 1/2 times as long as its middle width. In state (2), the male ectoproct is greater than 5 times as long as its middle width.

3.2.3 Molecular Characters

Partial sequences of two ribosomal genes are included and analyzed here, representing the mitochondrial (16S) and nuclear (18S) genomes. Both genes have recently been used to investigate the phylogenetic relationships between and within insect groups at various taxonomic levels (Anderson et al. 2010, Carr et al. 2010, Danforth et al. 2006, Dumont et al. 2010, Han & Ro 2009), including several studies with representatives in the order Neuroptera (Cameron et al. 2009, Winterton 2003, Winterton et al. 2010).

3.2.4 DNA Extraction and PCR

Genomic DNA was extracted from adult specimens, preserved in 95% EtOH and stored in a freezer (-80˚C) housed in the TAMUIC, or from material loaned from other institutions. A sterile razor blade was used to remove one leg from each specimen by making a V-shaped incision in the thoracic body wall, to remove the leg and associated muscle tissue. Molecular voucher specimens were deposited in a freezer (-80˚C) housed in the TAMUIC. DNA extractions were conducted on the leg and associated muscle tissue using the Qiagen DNesy® Blood and Tissue Kit (Qiagen, Germantown, MD). Extractions precisely followed the Purification of Total DNA from Animal Tissues (Spin-Column Protocol) methodology detailed in the DNesy® Blood and Tissue Handbook, with the addition of 1.0 ml of yeast tRNA (Fisher Scientific, Pittsburgh, PA) during Step 3 to increase DNA precipitation and yield.

All purified DNA products were amplified by polymerase chain reaction (PCR) using 25 ul reactions consisting of the following reactants: 12.0 ul clean H_20, 10.0 ul Hot MasterMix (Fisher Scientific, Pittsburgh, PA), 1.0 ul forward primer, 1.0 ul reverse primer and 1.0 ul template DNA. Primer sequences used in this study were selected from Winterton et al. (2010), where they had been used successfully in the amplification of DNA from other neuropteran taxa, and are detailed in Table 3. 16S rDNA was amplified using a single primer pair, resulting in one fragment (ca. 525 bp), by the following PCR protocol: 95˚C for 3 min, 92˚C for 15 s, 48˚C for 45 s, 92˚C (5x) for 15 s, 92˚C for 15 s, 52˚C for 45 s, 65˚C for 2 min 30s, 92˚C (29x) for 15s, 65˚C for 7 min, 4˚C hold. Amplification of 18S rDNA was conducted using three primers pairs, resulting in three fragments (Region 1, ca. 700bp; Region 2, ca. 1100bp; and Region 3, ca. 900bp), by the following PCR protocol: 95˚C for 3 min, 95˚C for 1 min, 50˚C for 1 min, 65˚C for 2 min, 95˚C (30x) for 1 min, 65˚C for 7 min, 4˚C hold. For several 18S rDNA PCR reactions, the annealing temperature of 50˚C needed to be raised or lowered to achieve successful amplifications. The following taxa required a change in annealing temperature: Region 1- (51˚C) *P. hageni*, *H. fundata*, *C. annulata*, *M. mexicanus*, (52˚C) *P. congener*, *P. nevadensis*, *P. floridensis*, *V. fallax*, *M. texanus*, *N. bipennis*; Region 2- (45˚C) *M. mexicanus*; (51˚C) *P. congener*, *P. hageni*, *P. nevadensis*, *V. fallax*, *M. texanus*, *N. bipennis*; Region 3- (55˚C) *P. congener*, *P. nevadensis*, *H. fundata*, *C. annulata*, *M. texanus*, *M. mexicanus, N. bipennis*. PCR products were visualized using gel electrophoresis and cleaned using 1 ul Exosapit (Fisher Scientific) prior to sequencing. PCR products were submitted for Sanger DNA sequencing using the

Applied Biosystems Model 3130 Genetic Analyzer (Foster City, CA) at the Interdisciplinary Center for Biotechnology Research (University of Florida, Gainsville, FL). Forward and reverse primer sequence returns were assembled into contigs and edited using SEQUENCHER™ 4.1 (Gene Codes Corporation, Ann Arbor, MI). Contig sets (16S rDNA, 18S rDNA) for all taxa were compiled and formatted for alignment in Se-Al 2.0 (Rambaut 1996).

Table 3. Primer sequences used for PCR amplification and gene sequencing. Abbreviations: F, forward primer; MT, melting temperature; R, reverse primer; RG, region.

Primer (F/R)	Gene (RG)	Sequence	MT (˚C)
LR -J-12887(F)	16S	CCGGTTTGAACTCAGATCATGT	55.1
SR-N-13398 (R)	16S	CRCYTGTTTAWCAAAAACAT	47.0
20F (F)	18S (1)	CTGGTTGATCCTGCCAG	52.9
519R (R)	18S (1)	GWATTACCGCGGCKGCTG	58.1
Sia (F)	18S (2)	CCTGAGAAACGGCTACCACATC	57.6
Sbi (R)	18S (2)	GAGTCTCGTTCGTTATCGGA	53.8
18H (F)	18S (3)	GCTGAAACTTAAAGGAATTGACGGAAGGGCAC	62.5
18L (R)	18S (3)	CACCTACGGAAACCTTGTTACGACTT	58.6

Two different alignment strategies were implemented in order to investigate how each approach might affect the outcome of phylogenetic analyses. First, sequences were aligned using the Q-INS-I algorithm in MAFFT (Katoh et al. 2002, Katoh & Toh 2008). The Q-INS-i strategy is a search algorithm that utilizes the secondary structure information of RNA to construct multiple sequence alignments and has been shown to produce significantly better alignments than those of strictly sequence-based approaches (Letsch et al. 2008). Second, rDNA sequence data were aligned using the default

parameters in the program ClustalX v. 2.1 (Larkin et al. 2007). Datasets based on these two alignment strategies will be referred to as MAFQ and CLUX, respectively. Areas of uncertain alignment were removed from each alignment strategy using the default settings in the program Gblocks v. 091b (Castresana 2000). Gblocks uses several thresholds to define conserved regions in a multiple sequence alignment and concatenates these blocks into a final alignment that can be used in phylogenetic analyses. Datasets edited using this computerized exclusion method have been shown to produce tree topologies similar to those generated by the manual removal of variable alignment regions (Cameron et al. 2009) and result in less subjective, easier to reproduce final alignments.

3.2.5 Phylogenetic Analyses

Phylogenetic analyses were conducted on each sequence alignment (MAFQ and CLUX) using maximum parsimony (MP), maximum likelihood (ML) and Bayesian (BI) inference methods and on the morphological data matrix using only maximum parsimony. Fifteen different analyses were performed (Table 4) in order to investigate the effects of alignment strategy, data partitioning, and data type mixing (morphology and molecular) on the resulting phylogenies. jModelTest (Posada 2008, Guindon & Gascuel 2003) was used to determine the appropriate molecular model of sequence evolution for each gene (16S, 18S) separately and for both concatenated (16S + 18S) gene datasets. Model selection was conducted independently for MAFQ and CLUX alignments after removal of variable sequence regions with Gblocks. The GTR+G+I

model was selected by jModelTest for all concatenated gene datasets, under both the AIC and BIC criterion. However, due to the potential errors in estimating both the G and I parameters simultaneously (Yang 2006), the GTR+G model of molecular evolution was implemented for all concatenated gene dataset analyses using maximum likelihood and Bayesian methods. All analyses were conducted using both the GTR+G and GRT+G+I models to test for topology similarity, but only slight differences in clade support values (bootstrap or Bayesian posterior probabilities) were observed. All models selected by jModelTest for 16S and 18S alignments individually were not available to be implemented in either of the programs used for maximum likelihood and Bayesian analyses, therefore, a GTR+G model was also applied to all partitioned analyses using sequence data. For mixed datasets (morphological + molecular data) analyzed using Bayesian inference methods, morphological character parameters were set as unlinked and a gamma-shaped rate variation was enforced as suggested in the MrBayes v. 3.2 manual. All trees were visualized in FigTree (available at: http://tree.bio.ed.ac.uk/software/figtree/) and edited using Paint v. 6.1 (Microsoft Corporation, 2009).

Maximum parsimony (MP) analyses on morphology only (MORP), concatenated gene (MAFQ-MP, CLUX-MP) and concatenated mixed datasets (MAFQ-MP-MIX, CLUX-MP-MIX) were conducted using the "branch and bound" search option in PAUP* 4.0b10 (Swofford 2002). *Nemoptera bipennis* was manually set, using the "outgroup" command, as the root outgroup before conducting all analyses. Support values for clades recovered during MP analyses were generated by conducting 1000

Table 4. Details of datasets used for phylogenetic analyses and support values for recovered clades of interest. For maximum parsimony analyses, clade support is reported as a bootstrap value. For maximum likelihood analyses, clade support is reported as a rapid bootstrap value. For Bayesian inference methods, clade support is reported as a Bayesian posterior probability. Abbreviations: Acan = tribe Acanthaclisini; BI, Bayesian analysis; CLUX, ClustalX aligned (default settings); MAFQ, MAFFT aligned (Q-INS-I algorithm); MIX, mixed dataset (morphology and molecular characters); ML, maximum likelihood analysis; MORP, morphological characters only; MP, maximum parsimony analysis; PAR, partitioned analysis; Para, genus *Paranthaclisis*; Par+Vel , *Paranthaclisis and Vella*.

Dataset Name	Alignment	Data	Partition	Clade Support Values		
				Para	Par+Vel	Acan
MORP	N/A	Morphology only	None	70	<50	97
MAFQ-MP	MAFFT Q-INS-I	16S/18S	None	<50	<50	100
CLUX-MP	ClustalX default	16S/18S	None	59	53	100
MAFQ-MP-MIX	MAFFT Q-INS-I	16S/18S/morphology	None	75	62	100
CLUX-MP-MIX	ClustalX default	16S/18S/morphology	None	77	61	100
MAFQ-ML	MAFFT Q-INS-I	16S/18S	None	73	57	100
CLUX-ML	ClustalX default	16S/18S	None	83	65	100
MAFQ-ML-PAR	MAFFT Q-INS-I	16S/18S	By gene	86	73	100
CLUX-ML-PAR	ClustalX default	16S/18S	By gene	91	74	99
MAFQ-BI	MAFFT Q-INS-I	16S/18S	None	100	70	100
CLUX-BI	ClustalX default	16S/18S	None	100	90	100
MAFQ-BI-PAR	MAFFT Q-INS-I	16S/18S	By gene	99	86	100
CLUX-BI-PAR	ClustalX default	16S/18S	By gene	100	94	100
MAFQ-BI-MIX	MAFFT Q-INS-I	16S/18S/morphology	By gene	100	96	100
CLUX-BI-MIX	ClustalX default	16S/18S/morphology	By gene	100	87	100

bootstrap (bs) replicates performed under the same "branch and bound" search strategy. Strict consensus trees were generated for all MP searches that returned more than one equally most parsimonious tree. Maximum likelihood (ML) analyses were performed using RaxML (Stamatakis 2006) as implemented in the raxmlGUI (Silvestro & Michalak 2011). Analyses of concatenated gene (MAFQ-ML, CLUX-ML) and concatenated partitioned datasets (MAFQ-ML-PAR, CLUX-ML-PAR) were conducted

using the ML search, which included 1000 rapid bootstrap (rbs) replicates with branch lengths. For partitioned maximum likelihood analyses, datasets were partitioned by gene (16S and 18S). The best scoring ML trees were reported for each RaxML analysis, after confirming that these topologies matched 50% majority consensus trees constructed from all trees returned. Concatenated gene datasets (MAFQ-BI, CLUX-BI), partitioned gene datasets (MAFQ-BI-PAR, CLUX-BI-PAR) and mixed morphology/sequence datasets (MAFQ-BI-MIX, CLUX-BI-MIX) were analysed using the Bayesian inference (BI) method in MrBayes v.3.1.2 (Ronquist & Huelsenbeck 2003). Concatenated gene datasets were analysed using the GTR+G model by two independent runs, with four chains (three hot and one cold), for 10 million generations with sampling every 1,000 generations. All analyses were run to completion, with convergence of the two independent runs assessed using Tracer v. 1.5 (Rambaut & Drummond 2007), AWTY (Wilgenbusch et al. 2008) and the average standard deviation of split frequencies and PSRF statistics in MrBayes. Tracer was used to visualize MCMC traces (to check for convergence of the two independent runs) and effective sample size (ESS) of individual parameters. Convergence of paired independent runs was also assessed in AWTY by plotting the posterior probabilities of splits using the “compare” analysis option. A burn-in of 1,500 samples (15%) was used for summarizing all parameters and trees. For

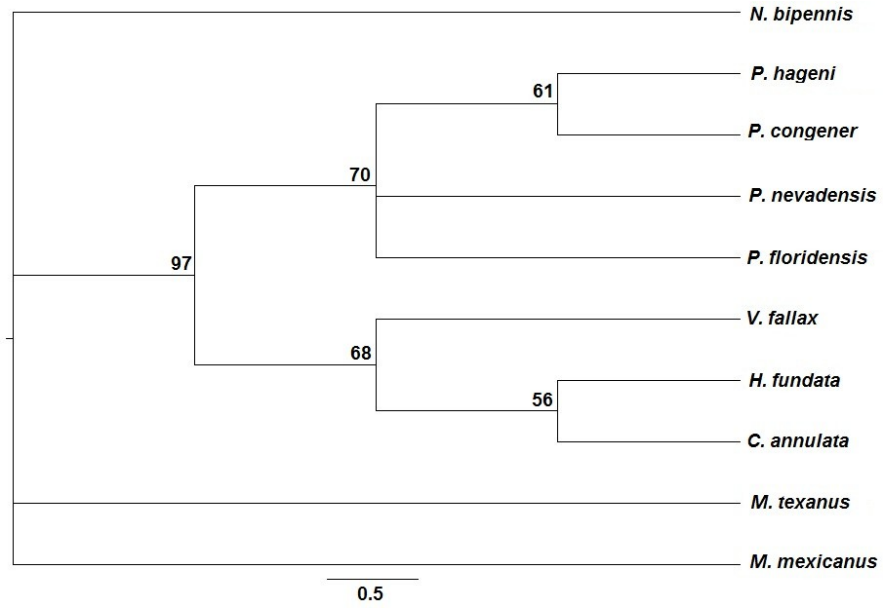

Figure 11. Strict consensus tree of maximum parsimony analysis of morphological only dataset (MORP) in PAUP*. Numbers at nodes are bootstrap values.

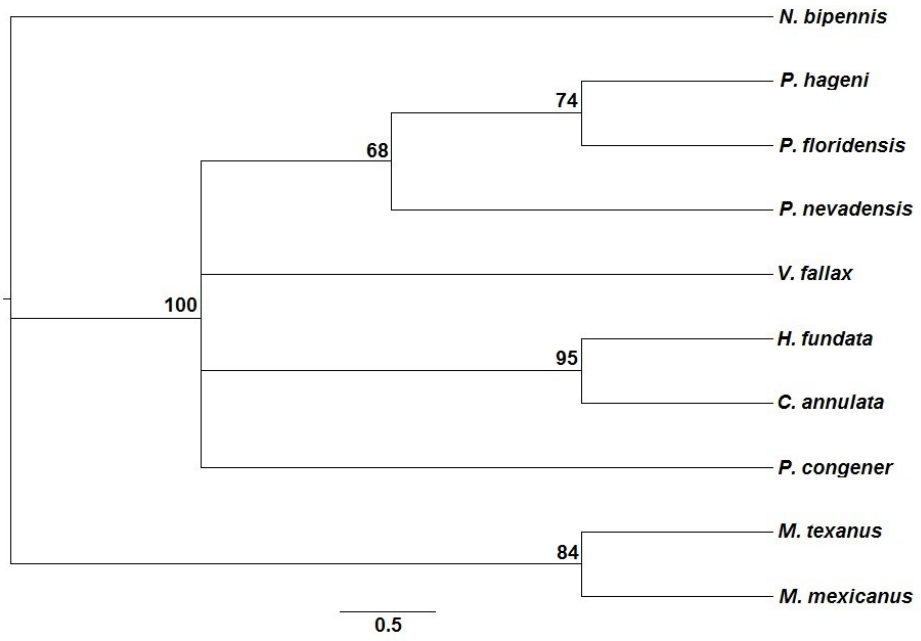

Figure 12. Strict consensus tree of maximum parsimony analysis of concatenated gene dataset (MAFQMP) in PAUP*. Numbers at nodes are bootstrap values.

partitioned and mixed Bayesian analyses, datasets were partitioned by gene (16S and 18S). 50% majority rule consensus trees were constructed for each analysis conducted in MrBayes and posterior probabilities (pp) reported for each clade.

3.3 Results

3.3.1 DNA Alignments

Use of the MAFFT Q-INS-i (MAFQ) strategy resulted in a 16S r-DNA multiple-sequence alignment of 509 characters and an 18S r-DNA alignment of 2629 characters. Multiple-sequence alignment in ClustalX (CLUX) resulted in the same 509 character 16S r-DNA alignment generated by MAFFT but a produced slightly shorter 18S r-DNA dataset of 2580 characters. After removal of highly variable aligned gene regions with Gblocks, the MAFQ and CLUX combined datasets were reduced to a length of 2511 (16S = 493, 18S = 2018) and 2589 (16S = 493, 18S = 2096) sequence characters, respectively.

3.3.2 Phylogenetic Analyses

Maximum parsimony analysis of the morphological dataset MORP returned nine trees of length 36. A strict consensus tree (fig. 11) supported the monophyly of the genus *Paranthaclisis* and the tribe Acanthaclisini with bootstrap support values of 70 and 97, respectively. The genus *Paranthaclisis* formed a sister-group to the remaining acanthaclisine genera included in the analysis. PAUP* MP analyses of concatenated gene datasets generated using different alignment programs did not produce identical

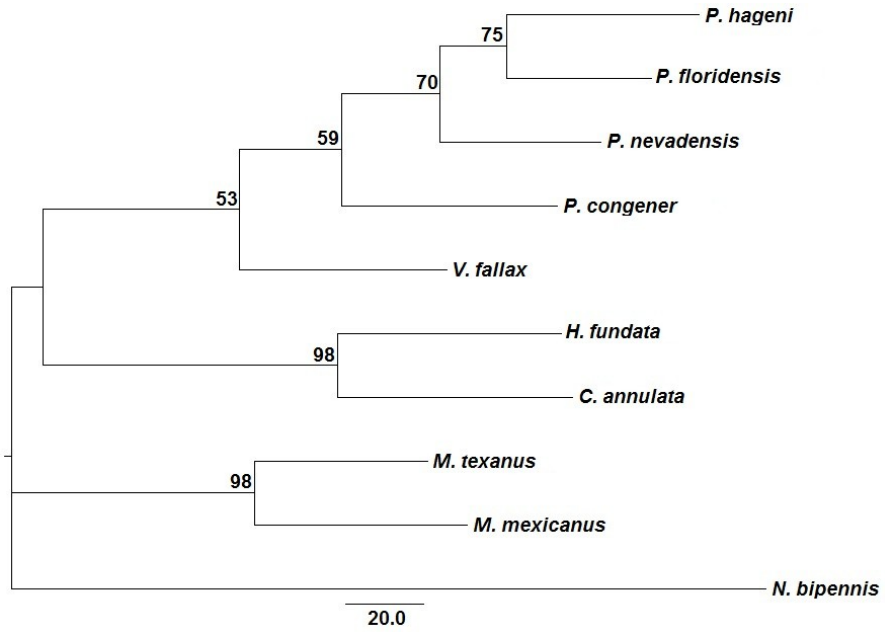

Figure 13. Single shortest tree of maximum parsimony analysis of concatenated gene/mixed datasets (CLUX-MP, MAFQ-MP-MIX, CLUX-MP-MIX) in PAUP*. Numbers at nodes are bootstrap values for the CLUX-MP dataset. See Table 4 for MAFQ-MP-MIX and CLUX-MP-MIX bootstrap values.

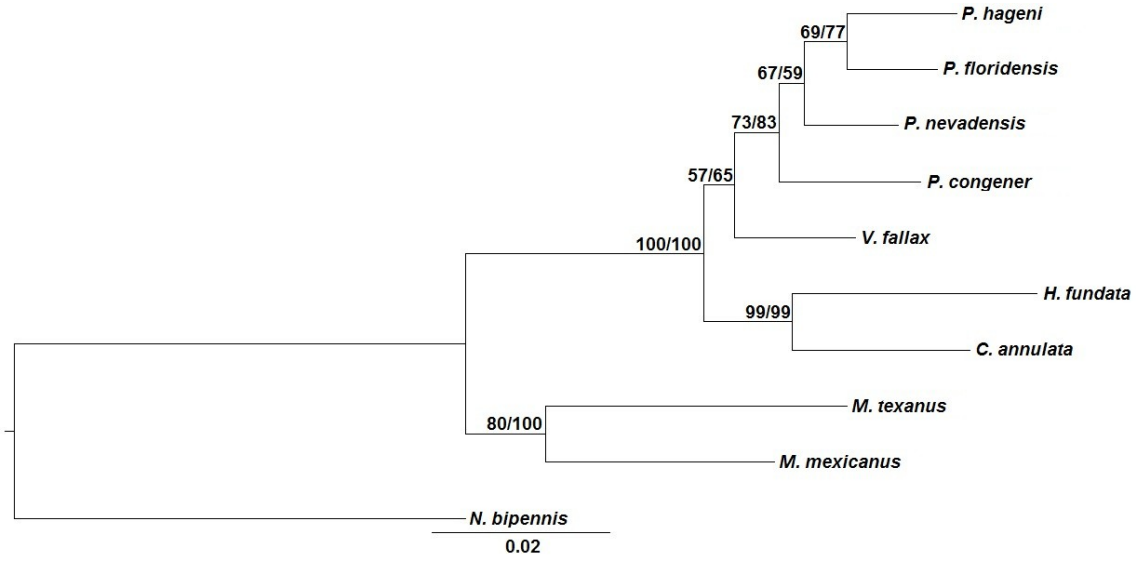

Figure 14. Best scoring tree of maximum likelihood analyses of unpartitioned gene datasets (MAFQ-ML, CLUX-ML) using RaxML. Numbers at nodes are rapid bootstrap values for the MAFQ-ML/CLUX-ML datasets.

tree topologies. The MAFQ-MP dataset found two trees of length 647 and the strict consensus (fig. 12) supported the monophyly of the tribe Acanthaclisini (bs = 100), but not the monophyly of the genus *Paranthaclisis*. The Old World acanthaclisine species *Heoclisis fundata* and *Cosina annulata* were recovered as sister taxa with high support (bs = 95). Only one shortest tree (length 729) was found using the CLUX-MP dataset (fig. 13), which had high support for the Acanthaclisini (bs = 100), but low support for both the monophyly of *Paranthaclisis* (bs = 59) and a sister-group relationship between the genus *Paranthaclisis* and *Vella fallax* (bs = 53). The clade *Heoclisis fundata* and *Cosina annulata* was recovered high support (bs = 98). A single most parsimonious tree was recovered for the MAFQ-MP-MIX (679 length) and CLUX-MP-MIX (764 length) datasets. Maximum parsimony analyses of these mixed datasets resulted in the same topology recovered from the CLUX-MP dataset (fig. 13), but with higher bootstrap support. Both the MAFQ-MP-MIX and CLUX-MP-MIX trees supported a monophyletic *Paranthaclisis* (bs = 75 and 77, respectively) and a monophyletic Acanthaclisini (bs = 100). A sister-group relationship between *Paranthaclisis* and *Vella* was recovered with lower support (bs = 62 and 61, respectively).

Unpartitioned maximum likelihood analyses using the MAFQ-ML and CLUX-ML datasets in RaxML returned the same 50% majority rule consensus trees (fig. 14), with only slight differences in rapid bootstrap values. Both the MAFQ-ML and CLUX-ML trees supported a monophyletic *Paranthaclisis* (rbs = 73 and 83, respectively) and a monophyletic Acanthaclisini (rbs = 100). A sister-group relationship between *Paranthaclisis* and *Vella* was recovered with low support (rbs = 57 and 65, respectively).

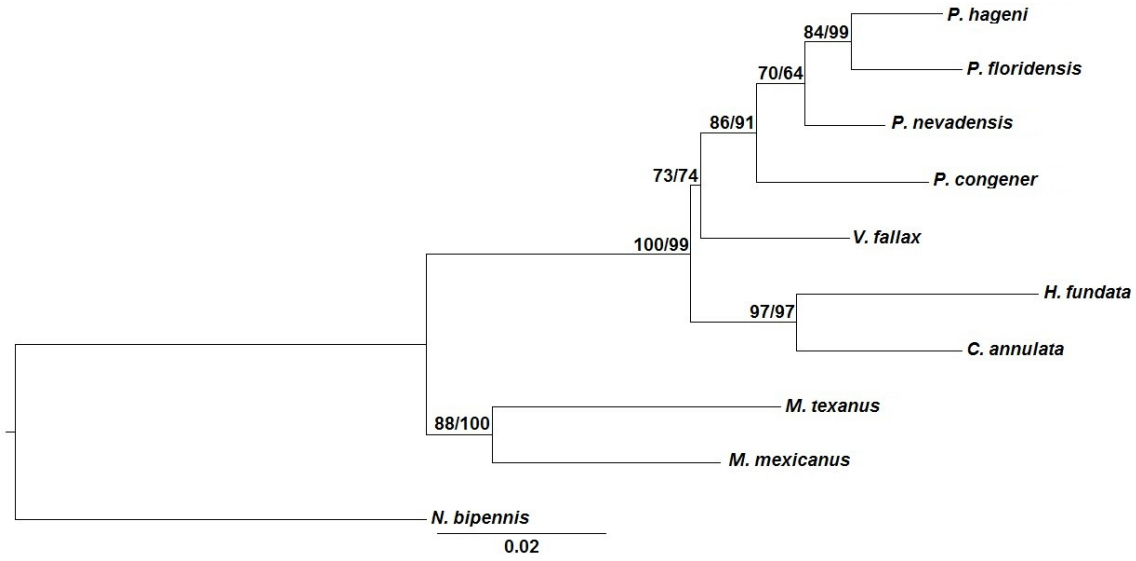

Figure 15. Best scoring tree of maximum likelihood analyses of partitioned gene datasets (MAFQ-ML-PAR, CLUX-ML-PAR) using RaxML. Numbers at nodes are rapid bootstrap values for the MAFQ-ML-PAR/CLUX-ML-PAR datasets.

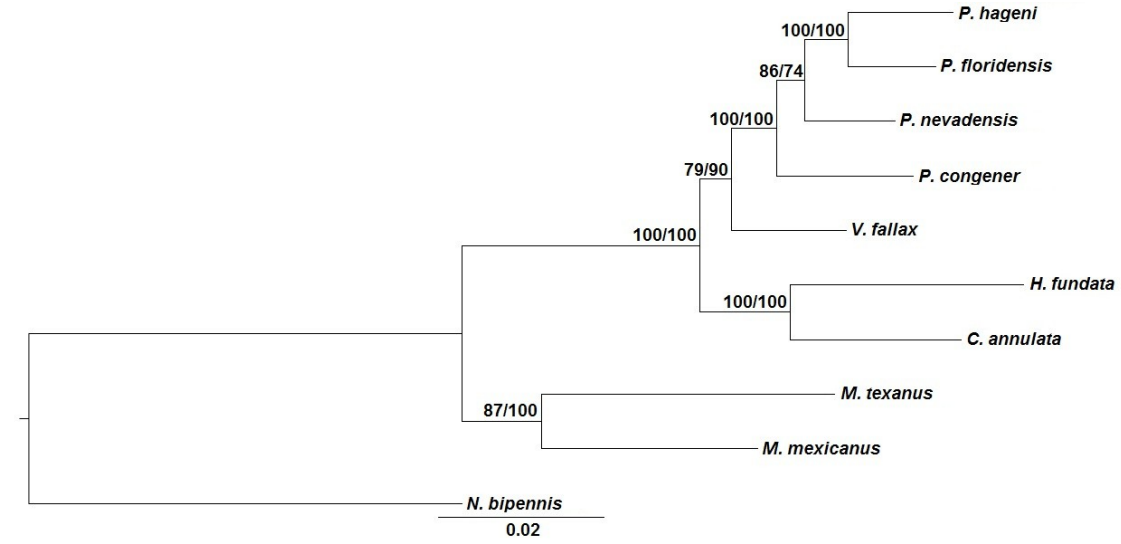

Figure 16. 50% majority rule consensus trees of Bayesian analyses of unpartitioned gene datasets (MAFQ-BI, CLUX-BI) using MrBayes. Numbers at nodes are Bayesian posterior probabilities for the MAFQ-BI/CLUX-BI datasets.

As in the MP analysis of the CLUX-MP dataset, both the MAFQ-ML and CLUX-ML datasets found the Old World acanthaclisine species *Heoclisis fundata* and *Cosina annulata* as sister taxa with high support (bs = 99). Maximum likelihood analyses partitioned by gene resulted in the same topology as the unpartitoned datasets but showed increased bootstrap support for several clades (fig. 15). In the MAFQ-ML-PAR and CLUX-ML-PAR analyses, support for both a monophyletic *Paranthaclisis* (rbs = 86 and 91, respectively) and a sister-group relationship between *Paranthaclisis* and *Vella fallax* (rbs = 73 and 74, respectively) was notably higher.

Bayesian inference methods returned similar topologies between the two different alignment methods, with only minor differences in posterior probabilities. For all datasets analysed, the average standard deviation of split frequencies was below the recommended value of 0.01 and PSRF values were equal to 1.00. Unpartitioned analyses in MrBayes, using the MAFQ-BI and CLUX-BI datasets, resulted in topologies (fig. 16) matching those recovered from ML searches using RaxML (fig. 14). Both topologies strongly supported a monophyletic *Paranthaclisis* (pp = 100) and monophyletic Acanthaclisini (pp = 100), as well as a moderately supported sister-group relationship between *Paranthaclisis* and *Vella* (pp = 70 and 90, respectively). Partitioned datasets recovered similar topologies but with generally higher posterior probabilities (fig. 17, main). The MAFQ-BI-PAR data matrix resulted in a topology similar to the unpartitioned MAFQ-BI, hoever, with the relationships between species in the genus

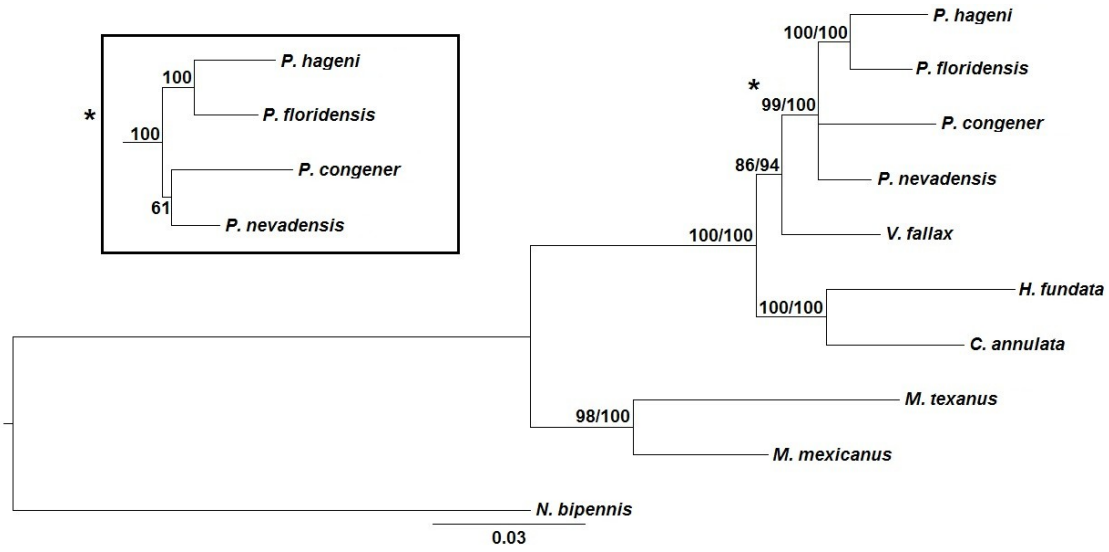

Figure 17. 50% majority rule consensus trees of Bayesian analyses of partitioned gene datasets (MAFQ-BI-PAR, CLUX-BI-PAR) using MrBayes. Numbers at nodes are Bayesian posterior probabilities for the MAFQ-BI-PAR/CLUX-BI-PAR datasets. An asterisk (*) denotes the topological difference resulting from analysis of the CLUX-BI-PAR dataset. Only slight differences in branch lengths were observed between the two datasets.

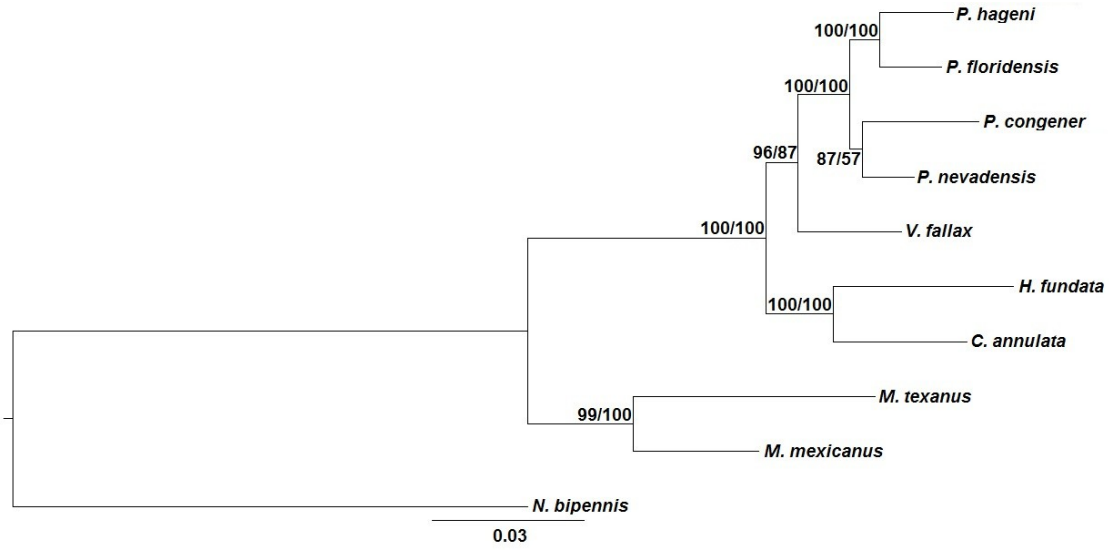

Figure 18. 50% majority rule consensus trees of Bayesian analyses of mixed datasets (MAFQ-BI-MIX, CLUX-BI-MIX) using MrBayes. Numbers at nodes are Bayesian posterior probabilities for the MAFQ-BI- MIX/CLUX-BI-MIX datasets. Only slight differences in branch lengths were observed between the two datasets.

Paranthaclisis being less resolved. In the partitioned analysis of MAFQ-BI-PAR, the genus *Paranthaclisis* forms a polytomy with *Paranthaclisis hageni* and *Paranthaclisis floridensis* recovered as sister taxa with high support (pp = 100). Support for the monophyly of the genus *Paranthaclisis* was slightly lower (pp = 99), but was muchhigher for a sister-group relationship between *Paranthaclisis* and *Vella fallax* (pp = 86). Analysis of the CLUX-BI-PAR dataset recovered a slightly different topology (fig. 17, inset) than MAFQ-BI-PAR, in the former of which the species relationships within *Paranthaclisis* are resolved, but differently than those found in the MP or ML analyses. As in the topology that resulted from the analysis of the MAFQ-BI-PAR dataset (fig. 17, main), *Paranthaclisis hageni* and *Paranthaclisis floridensis* are recovered as sister taxa with high support (pp = 100), but a sister-group relationship is also recovered between *Paranthaclisis congener* and *Paranthaclisis nevadensis* with low support (pp = 61). Partitioned analysis of the CLUX-BI-PAR dataset also recovered slightly higher support for the *Paranthaclisis* + *Vella* sister-group clade (pp = 94). Bayesian analyses using mixed datasets (morphology and molecular characters) recovered the same topology as found using the CLUX-BI-PAR dataset, but differed in clade support values (fig. 18). Analysis of the MAFQ-BI-MIX dataset showed high support for the monophyly of the genus *Paranthaclisis* (pp = 100) and for a sister-group relationship between *Paranthaclisis* and *Vella fallax* (pp = 96). Moderate support was recovered for the clade *Paranthaclisis congener* + *Paranthaclisis nevadensis* (pp = 87). The same topology was found using the CLUX-BI-MIX dataset as for the CLUX-BI-PAR dataset, but with

lower support for the sister-group relationships between *Paranthaclisis* and *Vella* (pp = 87) and between *Paranthaclisis congener* and *Paranthaclisis nevadensis* (pp = 57).

3.4 Discussion

All or a strong majority of phylogenetic analyses conducted for this study provided support for tree topologies in which the following groups are monophyletic: (1) Acanthaclisini, (2) *Paranthaclisis* + *Vella fallax*, and (3) *Paranthaclsis*. The monophyly of the genus *Paranthaclisis* is well supported in most ML (rbs = 73-91) and BI (pp = 99-100) analyses. Maximum parsimony analyses show moderate support (bs = 59-77) for a monophyletic *Paranthaclisis*. Only one analysis (using the MAFQ-MP dataset) did not recover a monophyletic *Paranthaclisis* (fig. 2). This maximum parsimony analysis used the concatenated gene dataset aligned using the Q-INS-I alignment strategy in the program MAFFT. Maximum parsimony analyses using the MORP, CLUX-MP, MAFQ-MP-MIX and CLUX-MP-MIX datasets did recover a monophyletic *Paranthaclsis,* but with moderate to low clade support (bs = 59, 70, 75 and 77, respectively). Only two analyses (using the MORP and MAFQ-MP datasets) did not recover a monophyletic sister-group relationship between the genus *Paranthaclisis* and *Vella fallax*. Both of these maximum parsimony analyses failed to recover this clade in strict consensus trees generated from multiple trees of equal length (MORP = nine trees, MAFQ-MP = 2 trees). Maximum parsimony analysis using the CLUX-MP, MAFQ-MP-MIX and CLUX-MP-MIX datasets (fig. 3) recovered the sister relationship between the genus *Paranthaclisis* and *Vella fallax* with low support (bs = 53, 62 and 61, respectively). One

of the two possible parsimony trees for the MAFQ-MP dataset recovered both the monophyly of the genus *Paranthaclisis* and the sister-group relationship between *Paranthaclisis* and *Vella fallax*, but these relationships were lost in constructing the strict consensus tree. The relationships among *Paranthaclisis* species differ among phylogenetic inference methods and partitioned datasets, except that *Paranthaclisis hageni* and *Paranthaclisis floridensis* always form a monophyletic group. It is interesting to note that Stange & Miller (2012) suggested that *P. hageni* and *P. floridensis* are the most similar *Paranthaclisis* species based on morphology. In all analyses conducted, the tribe Acanthaclisini was recovered as monophyletic with high clade support values (bs = 97-100, rbs = 99-100, pp = 100). The low bootstrap support for many clades resulting from maximum parsimony analyses can be attributed to the low number of morphological characters available for resampling in the MORP dataset, as well as the lack of a molecular model to properly account for the evolutionary history of sequence data (Felsenstein 2004). Such models are available for use in maximum likelihood and Bayesian inference methods and their use in this study resulted in similar topologies that had higher support compared to MP analyses.

Analysis of 13 of 15 datasets recovered a sister-group relationship between *Paranthaclisis* and *Vella fallax*. *Paranthaclisis* and *Vella* represent the only two New World acanthaclisine genera. In the majority of analyses, therefore, there is evidence for the reciprocal monophyly of the New World (*Paranthaclisis* and *Vella*) and Old World (*Heoclisis* and *Cosina*) genera of the antlion tribe Acanthaclisini. This hypothesis is supported by the current distribution of these groups, but this clade was not supported in

MP analysis of the MORP or MAFQ-MP datasets, and the current analyses are limited to four of the sixteen currently-recognized genera in the Acanthaclisini. Based on morphology of adults and larvae, Stange & Miller (1985) suggested that some New World acanthaclisine genera may be allied with Old World groups, including *Paranthaclisis* (with *Centroclisis*) and *Vella* (with *Heoclisis*). The grouping of *Vella+Heoclisis* was not recovered in any phylogenetic analyss in this study; however, a clade consisting of *Vella + (Heoclisis+Cosina)* was found in the MP analysis of the MORP dataset (fig. 11).

In this study, the choice of phylogenetic inference method and inclusion of partitions for gene datasets appeared to have the most influence on the topologies and clade support values for the resulting trees. Cameron *et al*. (2009) also found that using different inference methods (MP and BI) had the strongest influence on the topologies and suggested that was most likely due to the gamma parameter included in their model of choice for Bayesian analyses, GTR+G+I. The lack of the gamma parameter in their MP analyses using a concatenated gene dataset resulted in conflicting trees that did not support a traditional topology for some insect groups. A similar problem has likely occurred in the concatenated gene datasets using MP inference methods in this study. Partitioning by genes resulted in topological changes in the Bayesian analyses of MAFQ-BI-PAR and CLUX-BI-PAR datasets (fig. 7). Analysis of the MAFQ-BI-PAR dataset resulted in a less resolved *Paranthaclisis*, and use of the CLUX-BI-PAR dataset recovered a clade consisting of *Paranthaclisis congener* and *Paranthaclisis nevadensis* that was not found using the MAFFT alignment strategy. Previous research by Rota

(2011) suggests that partitioning datasets generally leads to higher support for clades. For the majority of partitioned analyses conducted in this study, clade support values (bs, rbs and pp) were higher than in unpartitioned analyses of the same dataset.

Choice of alignment strategy did not often have a major impact on topology here, but did result in clade support values that were generally higher for CLUX datasets (Table 4). For example, Bayesian analysis of the MAFQ-BI dataset recovered moderate support (pp = 70) for a sister-group relationship between *Paranthaclisis* and *Vella,* while the clade was highly supported (pp = 90) using the CLUX-BI dataset. It is possible that larger effects of these different alignment strategies on resulting phylogenies may have been lost after using the program Gblocks to remove areas of alignment uncertainty. This program removed large portions from both sequence alignments and future studies could compare this method with unedited datasets or manual methods of sequence exclusion.

4. CONCLUSIONS

A comprehensive revision of the North American antlion genus *Paranthaclisis* recognized the following four species: *P. congener* (Hagen), *P. floridensis* Stange & Miller, *P. hageni* (Banks) and *P. nevadensis* Banks. Redescriptions, distribution maps and figures of diagnostic morphological characters are provided, as well as a key to adult *Paranthaclisis* species. *Paranthaclisis californica*, described by Navás (1922), is formally synonymized with *P. hageni* Banks and *P. californica* Navás (1920).

Morphological, molecular and mixed datasets analysed in this study converged on a common phylogeny that provides initial support for a monophyletic *Paranthaclisis* and Acanthaclisini. Molecular and mixed datasets also indicated a potential sister-group relationship between *Paranthaclisis* and the only other New World acanthaclisine genus, *Vella*. This study represents one of the first to explore the phylogenetic relationships of taxa within the family Myrmeleontidae using DNA sequence data. Current taxonomic classifications within the antlions have been based solely on morphological characters. Incorporating sequence data into future phylogenetic analyses will be important for testing these hypotheses of relationships between myrmeleontid groups. In order to fully investigate the phylogenetic relationships within *Paranthaclisis* and within the tribe Acanthaclisini, further phylogenetic analyses are needed with increased taxon sampling and a larger dataset consisting of new genes and novel morphological characters.

REFERENCES CITED

Allen, G. R.; Croft, D. B. 1985. Soil particle size and the pit morphology of the Australian ant-lions *Myrmeleon diminutus* and *M. pictifrons* (Neuroptera: Myrmeleontidae). Australian Journal of Zoology 33:863-874.

Anderson, J. C.; Wu, J.; Gruwell, M. E.; Gwiazdowski, R.; Santana, S. E.; Feliciano, N. M.; Morse, G.; Normark, B. B. 2010. A phylogenetic analysis of armored scale insects (Hemiptera: Diaspididae) based upon nuclear, mitochondrial, and endosymbiont gene sequences. Molecular Phylogenetics and Evolution 57:992-1003.

Banks, N. 1892. A synopsis, catalogue, and bibliography of the neuropteroid insects of temperate North America. Transactions of the American Entomological Society 19:327-373.

Banks, N. 1895. Some Mexican Neuroptera. Proceedings of the California Academy of Sciences 5:515-522.

Banks, N. 1899. A classification of the North American Myrmeleontidae. Canadian Entomologist 31:67-71.

Banks, N. 1904. Neuropteroid insects from New Mexico. Transactions of the American Entomological Society 30:97-110.

Banks, N. 1907a. A new genus and a new species of Neuroptera. Entomological News, Philadelphia 18:275.

Banks, N. 1907b. Catalogue of the neuropteroid insects (except Odonata) of the United States. American Entomological Society, Philadelphia. 53 pp

Banks, N. 1911. Notes on African Myrmeleonidae. Annals of the Entomological Society of America 4:1-31.

Banks, N. 1913. Notes on African Myrmeleonidae. Journal of the New York Entomological Society 21:149-157.

Banks, N. 1927. Revision of the Nearctic Myrmeleonidae. Bulletin of the Museum of Comparative Zoology 68:1-84.

Banks, N. 1939. On some new and previously-known Neuroptera in the collection of the Academy of Natural Sciences of Philadelphia. Notulae Naturae 32:1-5.

Banks, N. 1942. Contributions toward a knowledge of the insect fauna of Lower California. No. 4. Neuroptera: Myrmeleonidae. Proceedings of the California Academy of Sciences 24:133-151.

Bezzi, S.; Kessler, D.; Diezel, C.; Muck, A.; Anssour, S.; Baldwin, I. T. 2010. Silencing NaTPI expression increases nectar germin, nectarins and hydrogen peroxide levels and inhibits nectar removal from plants in nature. Plant Physiology 152:2232-2242.

Cameron, S. L.; Sullivan, J.; Song, H.; Miller, K. B.; Whiting, M. F. 2009. A mitochondrial genome phylogeny of the Neuropterida (lace-wings, alderflies and snakeflies) and their relationship to the other holometabolous insect orders. Zoologica Scripta 38:575-590.

Carmean, D.; Kimsey, L. S.; Berbee, M. L. 1992. 18S rDNA sequences and the holometabolous insects. Molecular Phylogenetics and Evolution 1:270-278.

Carr, M.; Young, J. P. W.; Mayhew, P. J. 2009. Phylogeny of bethylid wasps (Hymenoptera: Bethylidae) inferred from 28S and 16S rRNA genes. Insect Systematics & Evolution 41:55-73.

Castresana, J. 2000. Selection of conserved blocks from multiple alignments for their use in phylogenetic analysis. Molecular Biology and Evolution 17:540-522.

Clinebell, II, R. R.; Crowne, A.; Gregory, D. P.; Hoch, P. C. 2004. Pollination ecology of *Gaura* and *Calylophus* (Onagraceae, tribe Onagreae) in western Texas, U.S.A. Annals of the Missouri Botanical Garden 91:369-400.

Currie, R. P. 1903. Myrmeleontidae from Arizona. Proceedings of the Entomological Society of Washington 5:272-284.

Danforth, B. N.; Sipes, S.; Fang, J.; Brady, S. G. 2006. The history of early bee diversification based on five genes plus morphology. Proceedings of the National Academy of Sciences 41:15118-15123.

Davis, D. R.; Milstrey, E. G. 1988. Description and biology of *Acrolophus pholeter*, (Lepidoptera: Tineidae), a new moth commensal from gopher tortise burrows in Florida. Proceedings of the Entomological Society of Washington 90:164-178.

Dias, S. C.; Santos, B. A.; Werneck, F. P.; Lira, P. K.; Carrasco-Carballido, V.; Fernandes, G. W. 2006. Efficiency of prey subjugation by one species of *Myrmeleon* larvae (Neuroptera: Myrmeleontidae) in the Central Amazonia. Brazilian Journal of Biology 66:441-442.

Dumont, H. J.; Vierstraete, A.; Vanfleteren, J. R. 2010. A molecular phylogeny of the Odonata (Insecta). Systematic Entomology 35:6-18.

Esben-Petersen, P. 1918. Results of Dr. E. Mjöberg's Swedish scientific expeditions to Australia 1910-1913. 18. Neuroptera and Mecoptera. Arkiv för Zoologi 11:1-37.

Felsenstein, J. 2004. Inferring Phylogenies. Sinauer Associates. Sunderland, MA. 664 pp.

Gepp, J. 2010. Ameisenlöwen und Ameisenjungfern. Myrmeleontidae. Eine weltweite Betrachtung unter besonderer Berücksichtigung Mitteleuropas. 3. neubearbeitete Auflage [3rd edition]. Die Neue Brehm-Bücherei 589. Westarp Wissenschaften-Verlagsgesellschaft, Hohenwarsleben. 168 pp.

Guindon, S.; Gascuel, O. 2003. A simple, fast, and accurate algorithm to estimate large phylogenies by maximum likelihood. Systematic Biology 52:696-704.

Hagen, H. A. 1860. Beitrag zur Kenntniss der Myrmeleon-Arten. Stettiner Entomologische Zeitung 21:359-369.

Hagen, H. A. 1861. Synopsis of the Neuroptera of North America, with a list of the South American species. Smithsonian Miscellaneous Collections 41:xx + 1-347.

Hagen, H. A. 1866. Hemerobidarum Synopsis synonymica. Stettiner Entomologische Zeitung 27:369-462.

Hagen, H. A. 1887. Stray notes on Myrmeleonidae, Part 2. Canadian Entomologist 19:133-136, 147-156.

Han, H.; Ro, K. 2009. Molecular phylogeny of the family Tephritidae (Insecta: Diptera): new insight from combined analysis of the mitochondrial 12S, 16S and COII genes. Molecules and Cells 27:55-66.

Haring, E.; Aspöck, U. 2004. Phylogeny of the Neuropterida: a first molecular approach. Systematic Entomology 29:415-430.

Hollis, K. L.; Cogswell, H.; Snyder, K.; Guillette, L. M.; Nowbahari, E. 2011. Specialized learning in antlions (Neuroptera: Myrmeleontidae), pit-digging predators, shortens vulnerable larval stage. PLoS ONE 6(3)e17958:1-7.

Katoh, K.; Misawa, K.; Kuma, K.; Miyata, T. 2002. MAFFT: a novel method for rapid multiple sequence alignment based on fast Fourier transform. Nucleic Acids Research 30:3059-3066.

Katoh, K.; Toh, H. 2008. Recent developments in the MAFFT multiple sequence alignment program. Briefings in Bioinformatics 9:286-298.

Larkin, M. A.; Blackshields, G.; Brown, N. P.; Chenna, R.; McGettigan, P. A.; McWilliam, H.; Valentin, F.; Wallace, I. M.; Wilm, A.; Lopez, R.; Thompson, J. D.; Gibson, T. J.; Higgins, D. G. 2007. Clustal W and Clustal X version 2.0. Bioinformatics 23:2947-2948.

Letsch, H. O.; Kück, P.; Stocsits, R. R.; Misof, B. 2008. The impact of rRNA secondary structure consideration in alignment and tree reconstruction: simulated data and a case study on the phylogeny of hexapods. Molecular Biology and Evolution 24:1-30.

Mansell, M. W. 1985. The ant-lions of southern Africa (Neuroptera: Myrmeleontidae). Introduction and genus *Bankisus* Navás. Journal of the Entomological Society of Southern Africa 48:189-212.

Markl, W. 1954. Vergleichend-morphologische Studien zur Systematik und Klassifikation der Myrmeleoniden (Insecta, Neuroptera). Verhandlungen der Naturforschende Gesellschaft in Basel 65:178-263 [Errata: 66:140].

McClure, M. S. 1976. Spatial distribution of pit-making ant lion larvae (Neuroptera: Myrmeleontidae): density effects. Biotropica 8:179-183.

Miller, R. B.; Stange, L. A. 1983. The ant-lions of Florida. *Glenurus gratus* (Say) (Neuroptera: Myrmeleontidae). Florida Department of Agriculture and Consumer Services, Division of Plant Industry, Entomology Circular 251:1-2.

Miller, R. B.; Stange, L. A. 1989. Revision of the genus *Dimarella* Banks (Neuroptera: Myrmeleontidae). Insecta Mundi 3:11-40.

Miller, R. B.; Stange, L. A. 2009. A revision of the genus *Maracandula* Currie (Neuroptera: Myrmeleontidae). Insecta Mundi 101:1-10.

Morris, J. M. 1997. El Llano Estacado: exploration and imagination on the High Plains of Texas and New Mexico. Texas State Historical Association 414:311-324.

Napolitano, J. 1998. Predatory behavior of a pit-making antlion, *Myrmeleon mobilis* (Neuroptera: Myrmeleontidae). Florida Entomologist 81:562-566.

Navás, L. 1912. Notas sobre Mirmeleónidos (Ins. Neur.). Brotéria (Zoológica) 10:29-75, 85-97.

Navás, L. 1919-1920. Sur des Névroptères nouveaux ou critiques. Deuxième [II] série. Annales de la Société Scientifique de Bruxelles 39(pt. 2):189-203.

Navás, L. 1922. Insectos nuevos o poco conocidos [I]. Memorias de la Real Academia de Ciencias y Artes de Barcelona 17:383-400.

New, T. R. 1981. Presence of hair-pencils in acanthaclisine antlions (Neuroptera: Myrmeleontidae). International Journal of Insect Morphology and Embryology 10:373-375.

New, T. R. 1985a. A revision of the Australian Myrmeleontidae (Insecta: Neuroptera). I. Introduction, Myrmeleontini, Protoplectrini. Australian Journal of Zoology, Supplementary Series 104:1-90.

New, T. R. 1985b. A revision of the Australian Myrmeleontidae (Insecta: Neuroptera). II. Dendroleontini. Australian Journal of Zoology, Supplementary Series 105:1-170.

New, T. R. 1985c. A revision of the Australian Myrmeleontidae (Insecta: Neuroptera). III. Distoleontini and Acanthaclisinae. Australian Journal of Zoology, Supplementary Series 106:1-159.

New, T. R. 1986. A review of the biology of Neuroptera Planipennia. Neuroptera International, Supplemental Series 1:1-57.

New, T. R. 1989. Planipennia, lacewings. Handbuch der Zoologie, Vol. 4 (Arthropoda: Insecta), Part 30. Walter de Gruyter, Berlin. 132 pp.

Nichols, S. W. (compiler); Schuh, R. T. (managing editor). 1989. The Torre-Bueno glossary of entomology. Revised Edition. New York Entomological Society, New York. 840 pp.

Oswald, J. D. 1993. Revision and cladistic analysis of the world genera of the family Hemerobiidae (Insecta: Neuroptera). Journal of the New York Entomological Society 101:143-299.

Oswald, J. D.; Contreras-Ramos, A.; Penny, N. D. 2002. Neuroptera (Neuropterida). Pp. 559-581 in Bousquets, J. L.; Morrone, J. J. (eds.). Biodiversidad, Taxonomía y Biogeografía de Artrópodos de México: hacia una síntesis de su conocimiento. Vol. 3. Universidad Nacional Autónoma de México, Distrito Federal, Mexico. x+690 pp.

Oswald, J. D. 2011. Bibliography of the Neuropterida: a bibliography and digital library of the literature of the extant and fossil Neuroptera, Megaloptera, and Raphidioptera (Insecta: Neuropterida) of the world. Version 9.00.

Penny, N. D. 1977. Lista de Megaloptera, Neuroptera e Raphidioptera do México, América Central, ilhas Caraíbas e América do Sul. Acta Amazonica 7(4)(Suplemento):1-61 [Errata: printed on a free slip of paper inserted in the work].

Penny, N. D.; Adams, P. A.; Stange, L. A. 1997. Species catalog of the Neuroptera, Megaloptera, and Raphidioptera of America north of Mexico. Proceedings of the California Academy of Sciences 50:39-114.

Posada, D. 2008. jModelTest: phylogenetic model averaging. Molecular Biology and Evolution 25:1253-1256.

Rambaut, A. E. 1996. Se-Al sequence alignment editor. University of Oxford, Oxford, U.K. Available at: http://evolve.zoo.ox.ac.uk/software/Se-Al.

Rambaut, A.; Drummond, A. J. 2007. Tracer v. 1.5. Available at: http://tree.bio.ed.ac.uk/software/tracer/.

Ronquist, F.; Huelsenbeck, J. P. 2003. MRBAYES 3: Bayesian phylogenetic inference under mixed models. Bioinformatics 19:1572-1574.

Rota, J. 2011. Data partitioning in Bayesian analysis: molecular phylogenetics of metalmark moths (Lepidoptera: Choreutidae). Systematic Entomology 36:317-329.

Silvestro, D.; Michalak, I. 2011. raxmlGUI: a graphical front-end for RAxML. Organisms, Diversity & Evolution DOI: 10.1007/s13127-011-0056-0.

Stamatakis, A. 2006. RAxML-VI-HPC: maximum likelihood-based phylogenetic analyses with thousands of taxa and mixed models. Bioinformatics 22:2688–2690.

Stange, L. A. 1961. Lectotype designations in the New World Myrmeleontidae. Canadian Entomologist 93:674-677.

Stange, L. A. 1970a. A generic revision and catalog of the western hemisphere Glenurini with the description of a new genus and species from Brazil (Neuroptera: Myrmeleontidae). Los Angeles County Museum, Contributions in Science 186:1-28.

Stange, L. A. 1970b. Revision of the ant-lion tribe Brachynemurini of North America (Neuroptera: Myrmeleontidae). University of California Publications in Entomology 55:vi+1-192.

Stange, L. A. 1980. The ant-lions of Florida. I. Genera. Florida Department of Agriculture and Consumer Services, Division of Plant Industry, Entomology Circular 215:1-4.

Stange, L. A. 1994. Reclassification of the New World antlion genera formerly included in the tribe Brachynemurini (Neuroptera: Myrmeleontidae). Insecta Mundi 8:67 - 119.

Stange, L. A. 2004. A systematic catalog, bibliography and classification of the world antlions (Insecta: Neuroptera: Myrmeleontidae). Memoirs of the American Entomological Institute 74:[iv]+565 pp.

Stange, L. A.; Miller, R. B. 1985. A generic review of the acanthaclisine antlions based on larvae (Neuroptera: Myrmeleontidae). Insecta Mundi 1:29-42.

Stange, L. A.; Miller, R. B. 2012. Description of a new species of *Paranthaclisis* Banks from Florida (Neuroptera: Myrmeleontidae). Insecta Mundi 224:1-5.

Stroud, C. P. 1950. A survey of the insects of White Sands National Monument, Tularosa Basin, New Mexico. American Midland Naturalist 44:659-677.

Swofford, D. L. 1999. PAUP*. Phylogenetic Analysis Using Parsimony (*and other methods), Version 4.0b4a. Sinauer Associates, Inc., Sunderland, Massachusetts.

Whiting, M. F.; Carpenter, J.C.; Wheeler, Q. D; Wheeler, W. C. 1997. The Strepsiptera problem: phylogeny of the holometabolous insect orders inferred

from 18S and 28S ribosomal DNA sequences and morphology. Systematic Biology 46:1-68.

Wilgenbusch, J.C.; Warren, D. L.; Swofford, D. L. 2008. AWTY (are we there yet?): a system for graphical exploration of MCMC convergence in Bayesian phylogenetics. Bioinformatics 24:581-583.

Winterton, S. L. 2003. Molecular phylogeny of Neuropterida with emphasis on the lacewings (Neuropterida). Entomologische Abhandlungen 61:158-160.

Winterton, S. L.; Hardy, N. B.; Wiegmann, B. M. 2010. On wings of lace: phylogeny and Bayesian divergence time estimates of Neuropterida (Insecta) based on morphological and molecular data. Systematic Entomology 35:349-378.

Yang, Z. 2006. Computational molecular evolution. Oxford University Press, Oxford, England. 376 pp.

Zack, R. S.; Penny, N. D.; Johnson, J. B.; Strenge, D. L. 1998. Raphidioptera and Neuroptera from the Hanford site of southcentral Washington state. Pan-Pacific Entomologist 74:203-209.

VITA

Name:	Benjamin Robert Diehl
Address:	Department of Entomology, Texas A&M University 412 Minnie Belle Heep Building, College Station, TX 77843-2475
Email Address:	b-diehl@tamu.edu
Education:	B.A., Entomology, The Ohio State University, 2010